Army Research Laboratory
Aberdeen Proving Ground, MD 21005-5069

ARL-TR-2471 **May 2001**

Application of Aluminum Foam for Stress-Wave Management in Lightweight Composite Integral Armor

Bruce K. Fink and Travis A. Bogetti
Weapons and Materials Research Directorate, ARL

Bazle Gama and John W. Gillespie, Jr.
University of Delaware

Chin-Jye Yu, T. Dennis Claar, and Harald H. Eifert
Fraunhofer USA

Abstract

Closed-cell aluminum foam offers a unique combination of properties such as low density, high stiffness, strength, and energy absorption that can be tailored through design of the microstructure. During ballistic impact, the foam exhibits significant nonlinear deformation and stress-wave attenuation. Composite structural armor panels containing closed-cell aluminum foam are impacted with 20-mm fragment-simulating projectiles (FSP). One-dimensional plane strain finite element analysis (FEA) of stress-wave propagation is performed to understand the dynamic response and deformation mechanisms. The FEA results correlate well with the experimental observation that aluminum foam can delay and attenuate stress waves. It is identified that the aluminum foam transmits an insignificant amount of stress pulse before complete densification. The ballistic performance of aluminum foam-based composite integral armor is compared with the base-line integral armor of equivalent areal density by impacting panels with 20-mm FSP. A comparative damage study reveals that the aluminum-foam armor has better and finer ceramic fracture and less volumetric delamination of the composite backing plate as compared to the base line. The aluminum-foam armors also showed less dynamic deflection of the backing plate than the base line. These attributes of the aluminum foam in integral armor system add a new dimension in the design of lightweight armor for the future armored vehicles.

Contents

INTENTIONALLY LEFT BLANK.

List of Figures

INTENTIONALLY LEFT BLANK.

List of Tables

INTENTIONALLY LEFT BLANK.

1. Introduction

The U.S. Army has established and documented requirements for lightweight structural armors that exhibit significant advancements in the integration of ballistic and structural performance [1]. Figure 1 depicts the historical development of armors for 0.50 cal. heavy machine gun threat demonstrating continuous improvements; yet, significant challenges exist in further reducing the areal density by half. Such a reduction in armor weight requires the integration of new materials, improved understanding of stress-wave propagation at dissimilar material interfaces, optimization of multiple competing performance metrics, and innovative armor concepts.

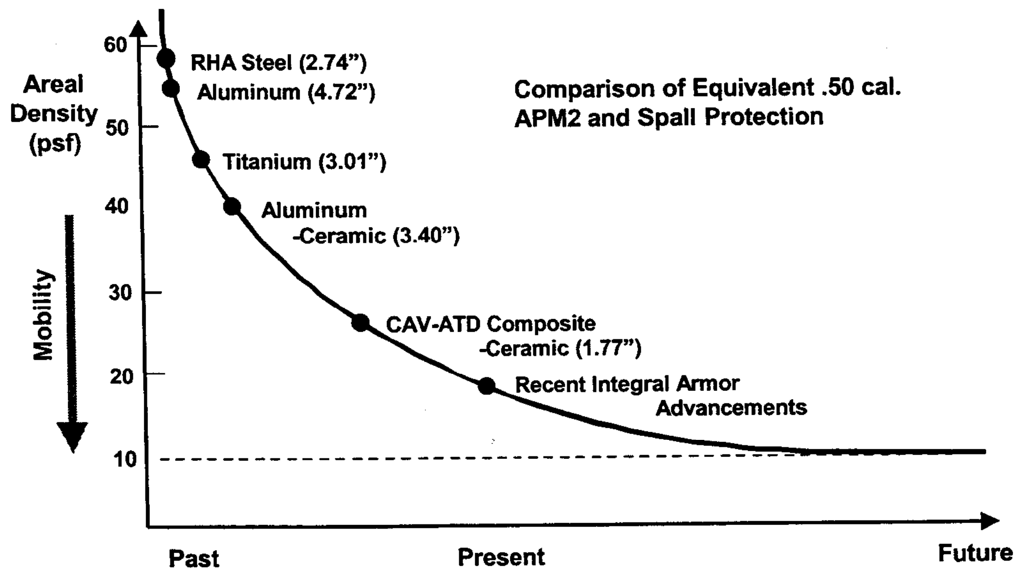

Figure 1. Historical development of composite integral armor.

One successful composite integral armor (CIA) developed by United Defertse Limited Partnership (UDLP) for the U.S. Army is a hybrid material system consisting of a ceramic strike face, a thin rubber layer, and an S-2 glass-based composite backing plate (Figure 2) [2]. This armor is required to provide ballistic protection and structural integrity at minimal areal density. Most CIA configurations utilize a rubber layer between the ceramic-tile layer and the composite-backing plate to increase the armor's multihit capability and structural damage tolerance [3, 4]. Experimental evidence shows that an increase in rubber layer thickness decreases the dynamic deflection of the composite backing plate [5]. One-dimensional numerical stress-wave experiments revealed

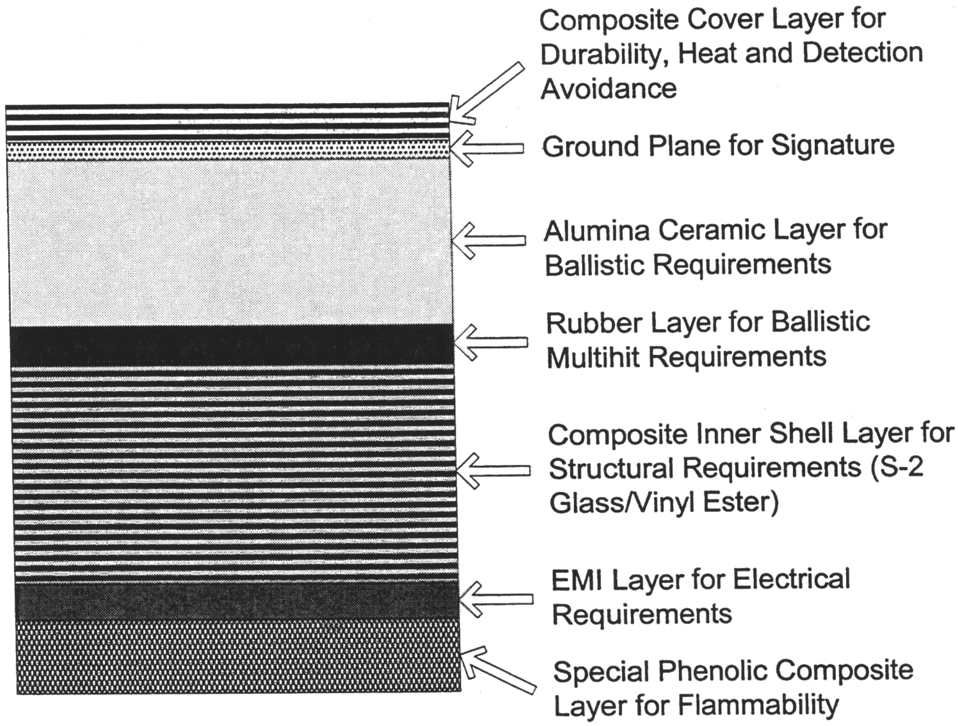

Figure 2. Components of integral armor structure.

that rubber delays the stress wave transfer and reduces the amplitude of transmitted stress wave to the backing plate [5]. The experimental and numerical results point to the importance of managing stress-wave propagation in CIA during ballistic impact. However, rubber is a compliant material and reduces the structural stiffness of the armor. Hence, an optimal rubber-layer thickness that balances the ballistic and structural performance at minimal weight should be determined to meet the specific mission requirements for a vehicle. Closed-cell aluminum foam is an alternative material to the rubber layer that has the potential to improve structural stiffness and ballistic properties. In the present study, we describe the stress-wave experiment through closed-cell aluminum foam, numerical stress-wave propagation models, design concepts, manufacturing and ballistic testing of a new generation of CIA.

2. Closed-Cell Aluminum Foam and Stress Wave Experiment

A variety of foaming processes and properties of closed-cell aluminum foam has been reported in the literature [6–10]. However, the foaming process via a powder metallurgy route produces a solid skin, which may be of interest especially for the surface bonding of another material, has high specific strength, and unique nonlinear compressive behavior [11]. Figure 3 shows the quasi-static engineering stress-strain behavior of such closed-cell aluminum foam of different densities (gm/cm^3). The flow stress of the foam is a strong function of foam density and the stress-strain curves can be divided into three regions—linear elastic region, collapse region, and densification region. In region 1, the only deformation that occurs is elastic and is due to cell-wall bending. This is followed by region 2 in which plastic collapse of the first cell wall occurs and the stress drops. In region 3, the foam progressively collapses and densifies. It was observed that deformation in region 3 was highly localized and proceeded by the advance of a densification front from deformed to undeformed regions of the sample. It has also been found that such a type of aluminum foams is essentially strain rate independent [11–12]. Hence the quasi-static properties of aluminum foam presented in Figure 3 are used in our numerical simulations.

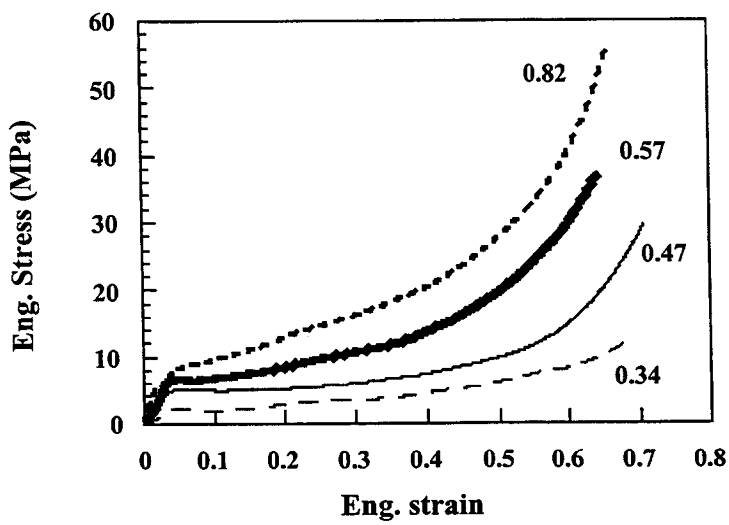

Figure 3. Quasi-static stress-strain behavior of closed-cell aluminum foam. Numbers on the figure represent foam density in gm/cm^3.

Ballistic targets with and without aluminum foam were designed and tested to compare the shock-wave propagation through the aluminum foam (Figures 4[a] and 4[b]). The target without aluminum foam had an areal-density of 161.03 kg/m^2 (32.98 psf) and the target with aluminum foam had an areal-density of 157.75 kg/m^2 (32.31 psf). High hardness steel (HHS), aluminum foam, alumina ceramic (Al_2O_3), and 7,039 aluminum plates are bonded together with a thin layer of fast-setting epoxy adhesive. Piezoresistant stress gages (Dynasen Model

Mn/Cn 4-50-EK) are sandwiched between two ceramic layers to monitor the dynamic stress through the ceramic layer. These gages consist of two separate interlaced 50-Ω foil grids enclosed in a polyamide plastic film. One of the grids is made of manganin and is used to measure stress. The other is made of constantan and is used to measure lateral strain. Both grids are 6.35-mm square and 0.127 mm thick. The measured strain is used to correct the stress measurements. The gages are connected to a Dynasen CK-15-300 power supply and bridge circuit, which is triggered upon projectile impact by a "make" screen with a simple capacitor discharge circuit. The signals from the gages are recorded on a digital oscilloscope. Calibration and data reduction of the stress gage signals are performed using software described by Franz and Lawrence [13]. Both the targets are impacted with 20-mm FSPs at a nominal impact velocity of 1,067 m/s. The stress gage measurements are presented in Figure 4(c). The rise time of the signal without foam is about 1.0 μs and with foam is about 2.0 μs. The maximum stress level attained in both the experiments is about 6.25 GPa. The incorporation of 12.7-mm aluminum foam delayed the stress signal about 14.6 μs to reach the gage location. We have developed a one-dimensional plane-strain finite element model of these experiments (detail of the model described in the following section) and have obtained about an 18.5-μs delay in the stress-wave arrival with an impact velocity of 500 m/s (Figure 4c). The finite element prediction also shows a two-step rise in stress in the case of target with aluminum foam. The stress waves generated in the experiments are a combination of spherical dilatation, spherical shear, and planar shear wave fronts. However, the plane-strain model only produces planar dilatation and is not an exact model of the experiment. The finite element model predictions capture both the widening in rise time and delay in stress-wave arrival. The experimental and finite element results identified two important characteristics of aluminum foam under stress-wave propagation: (1) aluminum foam increases the rise time of the propagating stress-wave, and (2) incorporation of aluminum-foam introduces a significant delay in stress-wave propagation. In order to determine the effect of aluminum-foam thickness, a second set of experiments is conducted.

The second set of stress-wave experiments deals with two ballistic targets with different aluminum foam thickness (12.7 mm and 30.48 mm) and is shown in Figure 5(a). An additional ceramic matrix composite layer (AS109, particulate SiC in Al_2O_3 matrix with a small amount of aluminum, made by Lanxide Armor Products) is bonded with the target described in Figure 4(b). The nominal impact velocity of a 20-mm FSP was 915 m/s. The projectile impact on the first target (Test # 1, with 12.7-mm aluminum foam) shattered the AS109 ceramic (Figure 5[b]), deformed the HHS plate, and densified the aluminum foam (Figure 5[c]). The stress gage recorded a stress pulse with the maximum stress

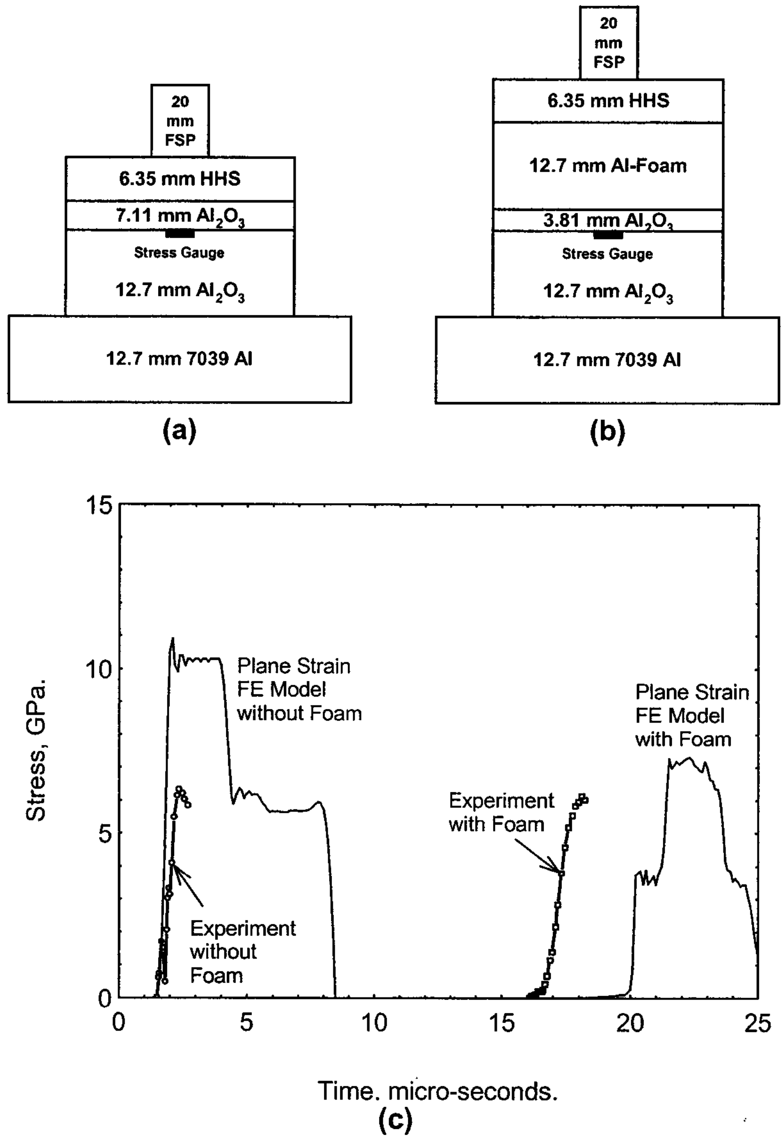

Figure 4. Stress wave experiment with and without aluminum foam (a) target without aluminum foam (b) target with aluminum foam (c) response of the stress gages and plane strain predictions.

amplitude of about 0.825 GPa. Impact on the second target (Test # 2, with 39.48-mm aluminum foam) showed similar fracture of AS109 ceramic and similar deformation of the HHS plate. However, the aluminum foam is partially densified (cross-section, Figure 5[d]), and the stress gage did not record any signal. The major conclusion from these two experiments is that if the foam is not completely densified across the entire layer thickness, it does not allow any measurable stress waves to pass through. The air/gas-filled cellular structure of the aluminum foam makes the stress-wave propagation difficult. The cell wall

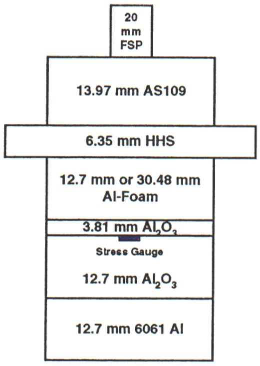

(a)

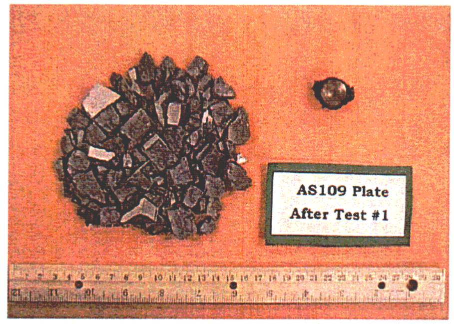

(b)

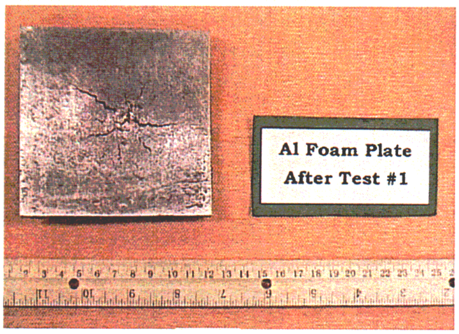

(c)

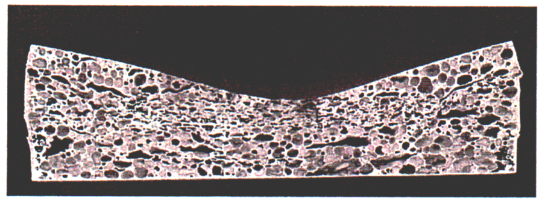

Al Foam Plate
After Test # 2

(d)

Figure 5. Stress wave experiment with different foam thickness (a) target with aluminum foam (b) fracture of AS109 ceramic strike face (c) deformation of aluminum foam after Test #1 (d) cross-section of the deformation of aluminum foam after Test #2.

acts as tiny wave-guide and dispersion of stress waves takes place. The deformation of closed-cell foam occurs by cell-wall buckling and plastic collapse, which leads to localized densification. The deformation and densification originates from the point of applied load and propagates in the direction perpendicular and transverse to the applied load. Effective stress-wave propagation can thus only occur when the closed-cell foam is completely densified. If the stress wave cannot reach the backing plate until the foam is completely densified, then the closed-cell foam has potential to improve the ballistic efficiency of the armor. A detailed finite element analysis of one-dimensional plane-strain stress-wave propagation in multilayer foam integral armor is presented next.

3. Stress Wave Propagation in Aluminum Foam Integral Armor

One-dimensional plane-strain stress-wave propagation in CIA and the effect of nonlinear EPDM rubber-layer thickness has been discussed by Gama et al. [5, 14]. One-dimensional plate impact produces planar dilatational stress-wave propagation in both the projectile and target. On the other hand, the impact of a three-dimensional (3-D) projectile (e.g., FSP) on a multilayer-thick armor plate produces 3-D spherical dilatational, spherical shear, and planar shear wave fronts. Since the dilatational wave speed is higher than the shear wave speed, the through-thickness stress-wave propagation in the impact centerline can be assumed planar, and our analyses are valid only in this region. The through-thickness and impact direction is assumed aligned with the coordinate axis z (3), and the in-plane axes are denoted by x and y (1 and 2). The rubber layer of the integral armor is replaced with an aluminum-foam layer (Figure 6). The individual layers are assumed perfectly bonded to each other. The thickness of the steel impact plate (5 mm), cover layer (2.54 mm), ceramic layer (17.78 mm), and the backing plate (14.15 mm) is kept constant throughout the analyses. The aluminum-foam layer thickness is varied between 12.7 mm and 25.4 mm. This combination of layer thicknesses represents an integral armor of areal density of about 97.65 kg/m^2 (20 psf). Linear elastic material properties are used to model the impact plate, cover layer, ceramic layer, and the backing plate (Table 1). The aluminum-foam is modeled with the MAT_HONEYCOMB material model within the explicit finite element code LS-DYNA 940, and the properties are extracted for foam density 0.57 gm/cc from Figure 3. The impact velocity of the steel plate is varied between 250 m/s to 750 m/s. The stress-wave propagation in the aluminum-foam armor is compared to armor without foam.

Figure 6 shows the deformation of aluminum-foam layer at different time intervals when impacted at 500 m/s. The plastic collapse and densification of foam starts at the impact side while the rest of the material remains elastic. It takes about 30 μs for the complete densification of 12.7-mm aluminum foam. The stress-wave propagation in the individual layers is a function of material properties and layer thickness. The dynamic response at midthickness of the individual layers is presented in Figure 7 as a function of time (aluminum-foam thickness = 12.7 mm, impact velocity = 500 m/s). Through-thickness normal stress is made nondimensional by the maximum compressive stress developed in the cover layer. The first compressive pulse in the cover layer is the input to the system. The stress in the cover layer becomes tensile as soon as the projectile bounces back from the target and the rest of the response is the reverberation of

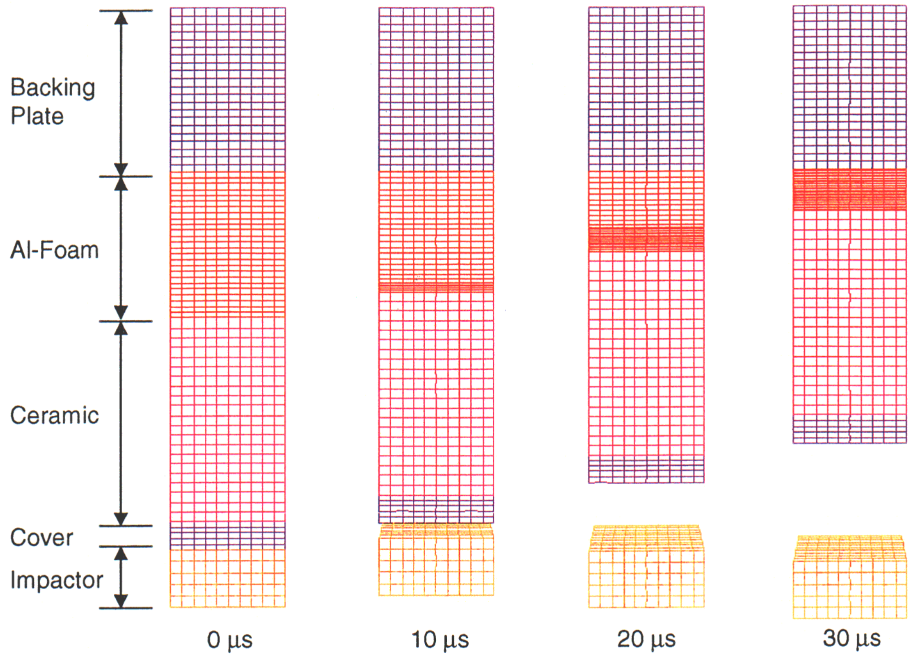

Figure 6. Plane strain finite element model of aluminum-foam integral armor and the dynamic deformation of the aluminum-foam layer.

Table 1. Material properties used in the one-dimensional finite element model.

Material	Young's modulus, E, GPa	Poisson's ratio, ν	Density, ρ, kg/m^3
Projectile	206.80	0.30	7850
Cover	8.50	0.28	1783
Ceramic	310.30	0.25	3500
Backing Plate	8.50	0.28	1783

	E,GPa	ρ, kg/m^3	Poisson's ratio of densified foam, $\nu_{densified}$	Yield stress, σ_y, MPa	Volume fraction of densified foam $v_{f,\ densified}$	Modulus of densified foam $E_{densified}$, GPa
Aluminum Foam	0.177	470	0.285	241.40	0.29	68.97

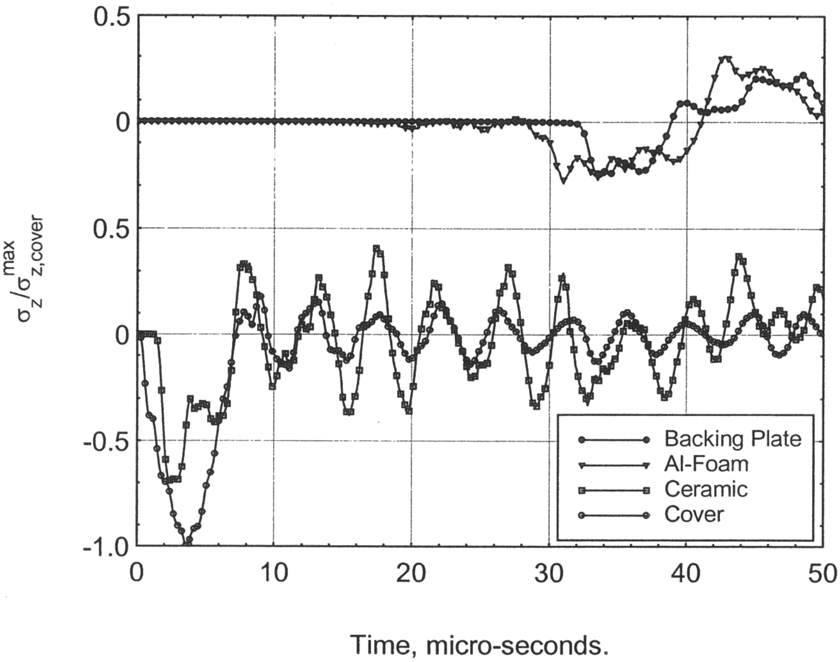

Figure 7. Dynamic response of individual layers, aluminum-foam thickness = 12.7-mm, impact velocity = 500 m/s.

the input pulse and the interaction with the adjacent ceramic layer. The input pulse in the cover layer is transmitted to the ceramic layer through the cover/ceramic interface. The transmission and reflection coefficients can be estimated using one-dimensional wave propagation theory [15]. The response of the aluminum foam layer and the backing plate is presented with a coordinate shift in stress. The transmission and reflection coefficients in the ceramic-foam interface are 0.0173 and -0.9827 respectively, which means that most of the compressive stress pulse will be reflected as tensile stress in the ceramic-foam interface before the collapse of aluminum foam. After the collapse and densification of aluminum foam layer (time > 26 μs), significant stress rise and propagation is observed in both the aluminum foam and backing plate. The maximum amplitude of the stress pulse transferred into the backing plate is about 25% of the input in the cover layer.

The response of aluminum foam (impact velocity = 500 m/s) as a function of layer thickness, *l*, is shown in Figure 8. The computation for foam thickness 12.7 mm and 19.1 mm was terminated at 50 μs and for 25.4 mm at 65 μs. The peak stresses are almost 25% of the input to the cover layer for all foam thicknesses. The stresses, however, become increasingly oscillatory with increased foam thickness. The arrival time of the stress pulse in the foam layer

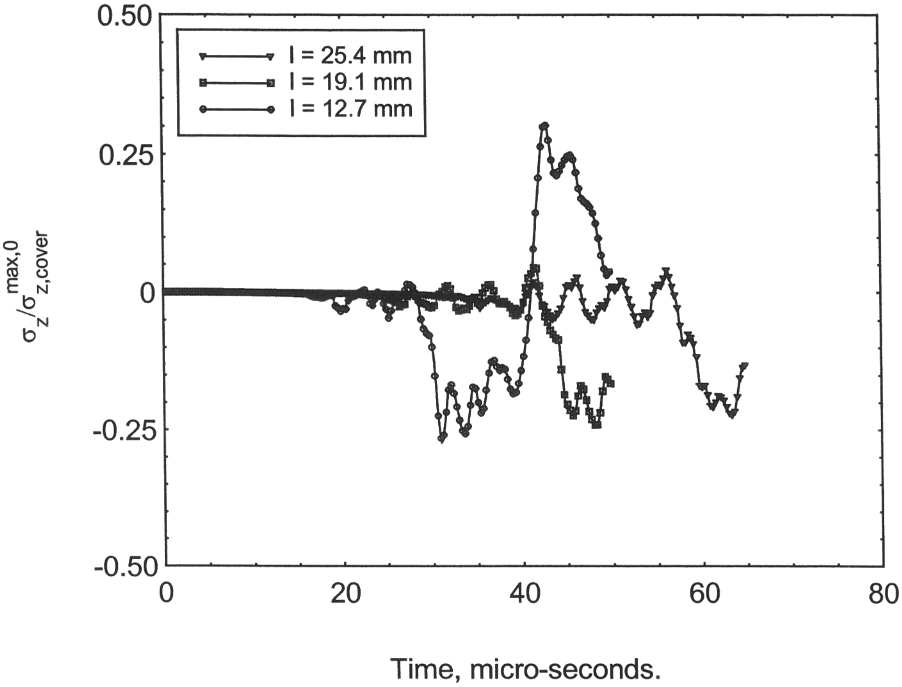

Figure 8. Dynamic response of aluminum-foam layer as a function of foam thickness, impact velocity = 500 m/s.

increases as a direct consequence of increased foam thickness and is related with the stress arrival at the backing plate (Figure 9). The solid line represents the response of backing plate without any foam (Figure 9a). The stress amplitude is found to decrease with the increase in foam thickness. The difference in the time of stress arrival to the backing plate with and without foam is termed as the time delay and increases with foam thickness. The peaks P, Q, and R in Figure 9a represent stress transfer to the backing plate after complete densification of the foam; however, a close-up shows earlier stress pulses (p, q, and r; Figure 9b) before the densification of foam and is termed as elastic stress transfer. The elastic stress transfer is less than 1% of input to the cover for all impact velocities studied (Figure 10). On the other hand, the stress transfer (for impact velocities 500 and 750 m/s) after complete foam densification linearly decreases at a rate of 1.1%/mm of foam thickness. The time delay of stress arrival in the backing plate is presented in Figure 11 and is found to be increasing with foam thickness. The time delay of elastic pulse for all impact velocities is about 0.75 μs/mm; however, the rate of time delay after foam densification decreases as impact velocity increases. These rates of delay are 2.16 and 1.42 μs/mm for impact velocities 500 and 750 m/s. At impact velocities higher than 750 m/s, the rate of delay approaches the rate of delay of the elastic pulse (0.75 μs/mm).

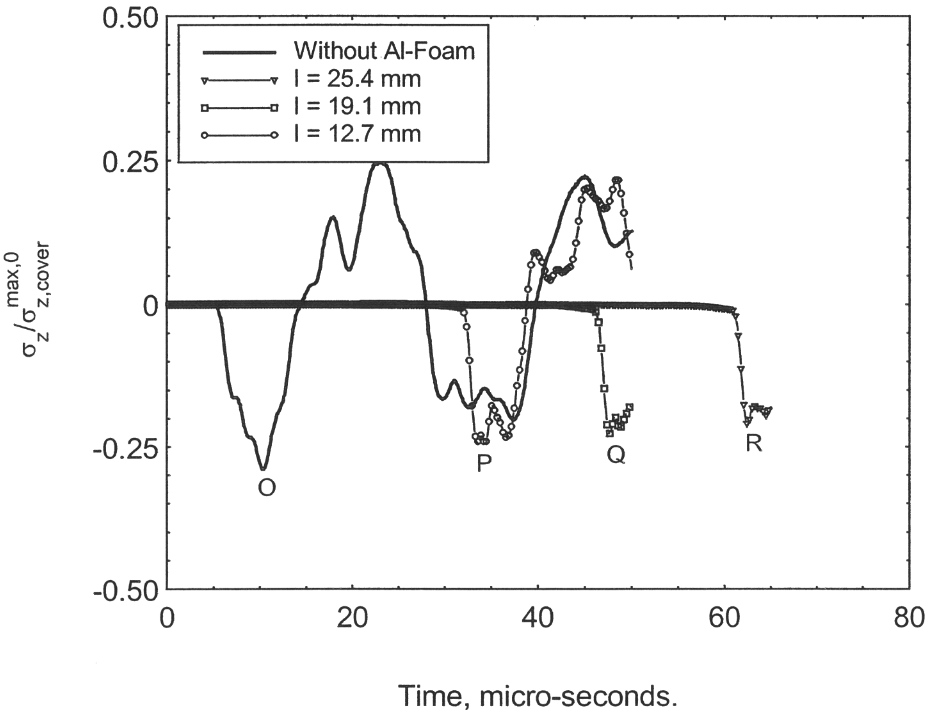

(a)

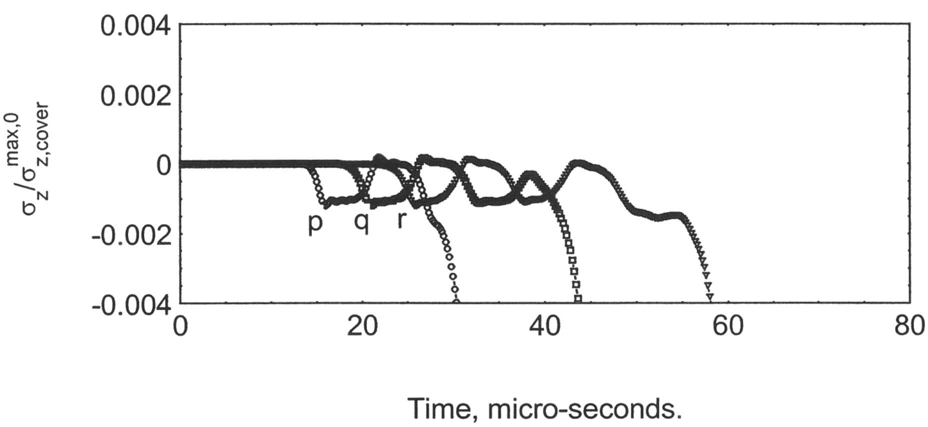

(b)

Figure 9. Dynamic response of the backing plate as a function of foam-layer thickness, impact velocity = 500 m/s, (a) effect of foam thickness (b) close-up of the response shows elastic response.

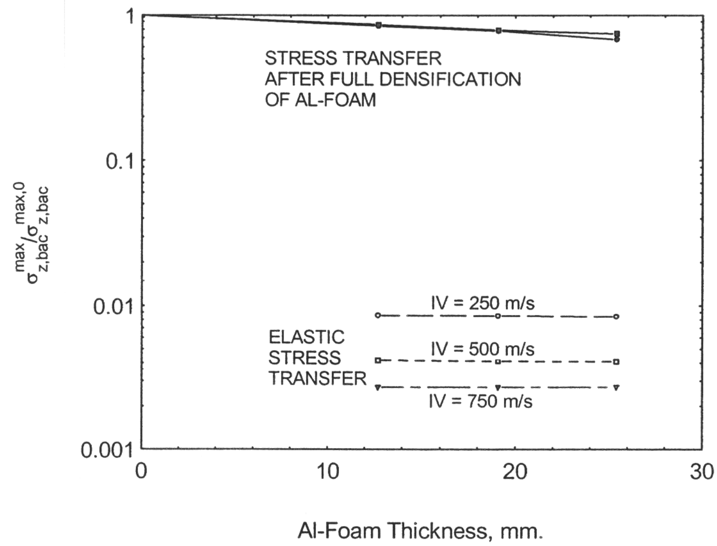

Figure 10. Transmission of stress pulse in the backing plate as a function of foam thickness.

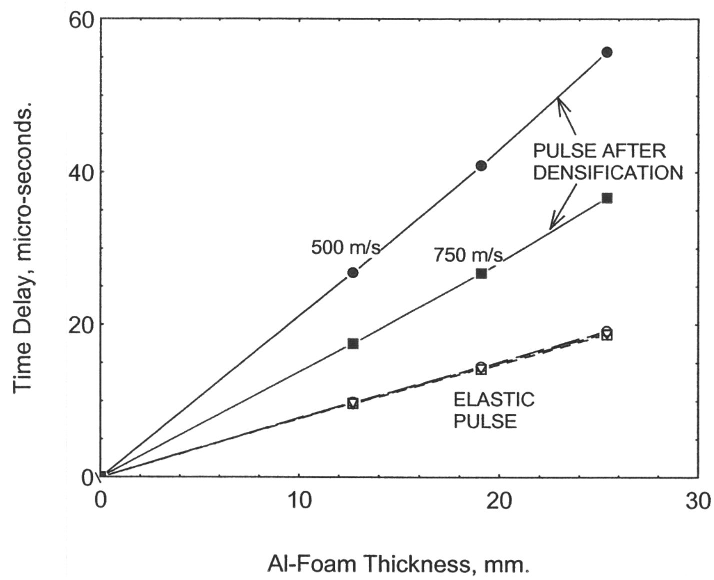

Figure 11. Time delay in the stress-wave arrival at the backing plate as a function of foam thickness.

As stated earlier, the one-dimensional stress analysis is valid at the impact centerline without penetration in the armor. In the real impact event, the penetration event follows the stress-wave propagation and the wave front is nonplanar. In order to investigate the penetration event, a quarter-symmetric three-dimensional model of aluminum foam integral armor impacted by a 20-mm FSP is developed. The foam layer thickness is taken as 19.1 mm. To mimic the stress-wave experiment done by Yu et al. [11], a thin layer of elastic-plastic material was incorporated in the model between the ceramic and aluminum foam layer. The initial impact velocity of the projectile is set to 900 m/s. The projectile and ceramic is modeled with MAT_PLASTIC_KINEMATIC and the backing plate is modeled with MAT_COMPOSITE_FAILURE_SOLID material models (Table 2). Figure 12 shows the sequence of projectile penetration and dynamic deformation of the aluminum foam. The solution is terminated after 63 μs because the foam cells are compressed down to infinitesimal thickness, and the time step required for such solution is so small that it takes infinite time to solve the problem. The cross-sectional view of the deformed aluminum foam [11] (Figures 5[d] and 13) shows that the deformation pattern obtained from the numerical simulation matches well with the experimental observation. The deformation pattern of the aluminum-foam also suggests that if an aluminum-foam plate is placed after the backing plate, it could contain the dynamic deflection of the armor.

Table 2. Material properties used in the three-dimensional finite element model.

Material	E, GPa	ν	ρ, kg/m^3	σ_y, MPa	Tangent modulus, E_t, GPa
FSP	206.91	0.285	7850	1069.1	2.0
Cover	20.00	0.22	1783	200.0	15.0
Ceramic	310.30	0.25	3500	3000.0	0.0

	E, GPa	ρ, kg/m^3	$\nu_{densified}$	σ_y, MPa	$\nu_{f,\ densified}$	$E_{densified}$, GPa
Aluminum Foam	0.177	470	0.285	241.40	0.29	68.97

	ρ, kg/m^3	Modulus, GPa		Poisson's ratio		Shear modulus, GPa	
Backing Plate	1783	E_{11}	29.48	ν_{21}	0.0085	G_{12}	3.79
		E_{22}	29.48	ν_{31}	0.1145	G_{23}	3.79
		E_{33}	29.48	ν_{32}	0.1145	G_{31}	3.79

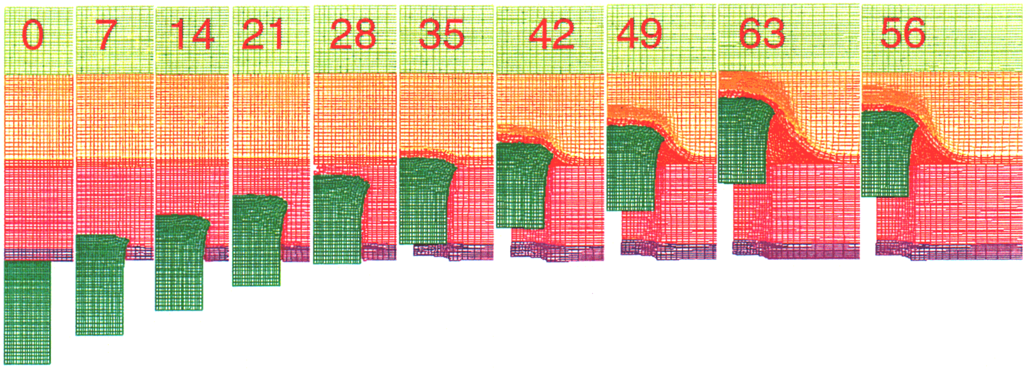

Figure 12. FE solution of dynamic deformation of aluminum-foam integral armor. Numbers indicate time in microseconds.

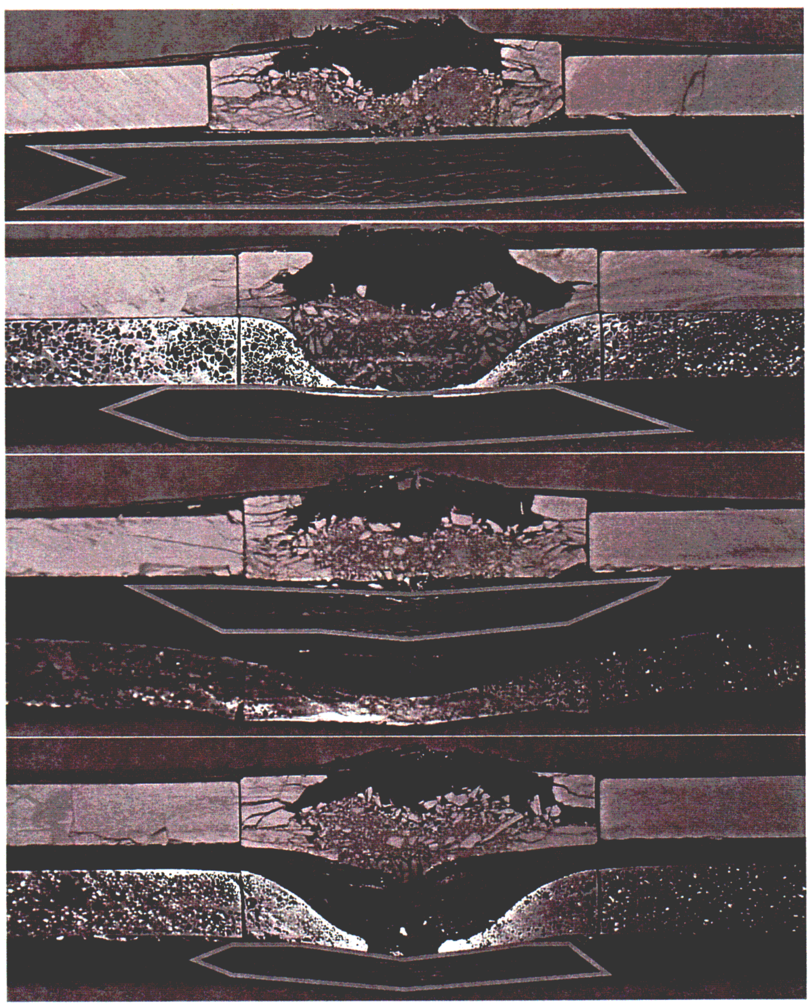

Figure 13. Impact damage modes of the aluminum-foam integral armor.

4. Design of Aluminum Foam Integral Armor

Based on the stress-wave experiment of Yu et al. [11] and the numerical simulation presented in section 3, a test matrix has been developed (Figure 14) to assess the potential benefits of using metal foams in an integral armor and to design the next generation integral armor to satisfy the Army requirements [1]. Three different designs of integral armor with metal foam have been proposed. These designs represent unique functionality of the aluminum foams in the integral armor. The rubber layer of the baseline CIA (Figure 14a, Baseline) has been simply replaced by the aluminum foam (Figure 14b, Design 1) to eliminate any relative rotational degrees of freedom between ceramic and backing plate, to improve structural stiffness of the armor, and to attenuate the stress-wave propagation. The next design (Figure 14c, Design 2) includes an additional aluminum foam backing plate to minimize dynamic deflection. The last design (Figure 14d, Design 3) uses a rubber layer and a thin composite inner layer to distribute the load over a greater region on the metal foam. The material system and individual layer thickness is marked on Figure 14. All designs have the same areal density of 97.65 kg/m^2 (20 lb/ft^2) as the base-line CAV integral armor. The thickness of the cover layer and the ceramic layer is kept constant for all design cases. The foam thickness is also kept constant at 19.00 mm to minimize the production cost of foam panels. If rubber is used in the foam armor panels, the thickness is chosen to be the same as the base line. The only parameter varied to keep the areal density constant is the backing plate thickness.

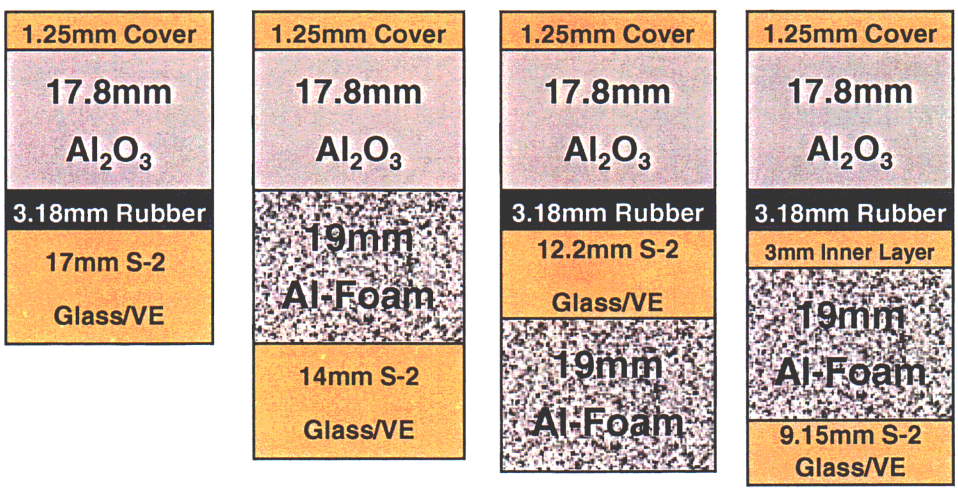

(a) Base line (b) Design 1 (c) Design 2 (d) Design 3

Figure 14. Innovative design of aluminum-foam integral armor.

5. Multistep Processing of Armor Panels

A total of four base-line armor panels and one of each aluminum foam CIA configuration is manufactured using a multistep manufacturing technique. This method is presented in Figure 15. The composite backing plates of different thicknesses are processed using vacuum-assisted resin-transfer molding (VARTM). Details of the VARTM process can be found [16]. Plain weave S-2 glass fabric (24 oz/yd^2) with 365-mm sizing is used to make the preforms. The preforms are infused with vinyl ester 411-C50 resin, cured at room temperature and postcured at 121 °C (250 °F) for 3 hr. The S-2 glass/vinyl ester panels are then machined to 305- × 305-mm size. EPDM rubber sheets of the same size are washed with soap and water and dried, and a thin coating of LORD 7701 primer is applied to both sides. Closed-cell aluminum-foam panels of nominal density 500 kg/m^3 and of dimension 101.6 × 101.6 × 19.0 mm were fabricated. The foam panels are cleaned with distilled water and dried at room temperature. A solution containing 10% glycidoxy (epoxy) functional methoxy silane (Dow Corning® Z-6040) is prepared with deionized water. Acetic acid is added to the solution to maintain pH in the 3.5–4.0 range. The aluminum foam panels are then soaked into the silane solution and oven dried for an hour at 90 °C. Hexagonal ceramic tiles (AD-90) are cleaned with compressed air. Nonhexagonal ceramic pieces required making a 305- × 305-mm-square array of tiles cut from the hexagonal tiles using a slot grinder. Fishing lines are cut into small pieces and bonded with spray adhesive on the sides of the ceramic tile to ensure a gap between adjacent tiles. The next step is to bond the individual layers with SC-11 epoxy resin. A wooden frame is made to hold all the layers together. A peel ply is used to avoid contact between the wooden mold and the part. The backing plate is first placed on the wooden frame. A thin layer of epoxy resin is then evenly distributed on top. To control the bond-line thickness, a glass scrim cloth (0.125 mm thick) is placed on the backing plate. More resin is added on top of the scrim cloth. The rubber (or aluminum foam) layer is laid next. On top of the rubber layer, resin and scrim cloth are placed to bond the next layer (ceramic layer or any successive layer). Once the hand lay-up of all layers is completed, the assembly is placed in a vacuum bag with sufficient breather material to absorb the excess epoxy resin. The vacuum bag is then placed inside an oven and the part is cured at 121 °C (250 °F) for 2 hr and at 149 °C (300 °F) for another 2 hr under vacuum. Once the cure is complete, the part is slowly cooled in the oven under vacuum. This armor plate is then covered with two layers of S-2 glass fabric and VARTM processed with vinyl ester 411-C50 resin at room temperature to obtain the cover layer. The complete integral armor is then postcured at 121 °C (250 °F) for 3 hr.

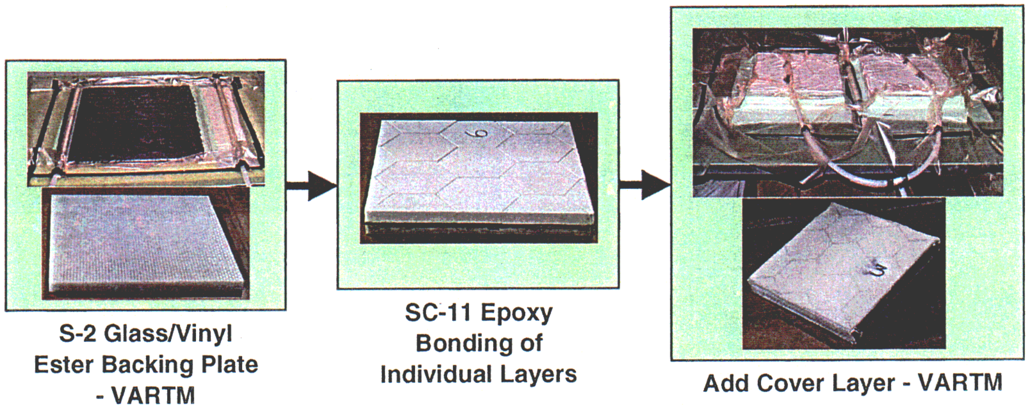

Figure 15. Multistep processing of integral armor.

6. Ballistic Testing of Armor Panels

Integral armor panels are impacted with 20-mm FSP projectiles. Previous research suggested that a 20-mm FSP with impact velocity of 838 m/s (2,750 ft/s) defeats a 97.6 kg/m^2 (20 lb/ft^2) CIA without penetrating the backing plate [3, 4]. Accordingly, all the impact tests were conducted at a nominal impact velocity of 838 m/s.

7. Ballistic Test Results and Discussion

Dynamic deflection of the back face of the armor under incomplete/partial penetration is a critical performance metric [1]. The integral armor panels were mounted on a thick backing of plasticine clay before projectile impact. The dynamic deformation of the back face of the armor is engraved in the plasticine clay after the impact event. This dynamic deflection is then measured as a function of radial location and is presented in Figure 16 for all the tests done. Dynamic deflection of the baseline CIA is presented with the error bars from four test specimens. The curve has a bell shape with a peak at about 32 mm (1.25 in) and a span diameter of about 200 mm (8.0 in). Design 1 has a dynamic deflection contour, which shows less deflection over the whole span as compared to the base line. Design 2 has the least dynamic deflection among all the armor panels tested. Design 3 has higher deflection in the central region but less over the rest of the span as compared to the base line. These observations are correlated with the deformation and damage profile presented in Figure 16.

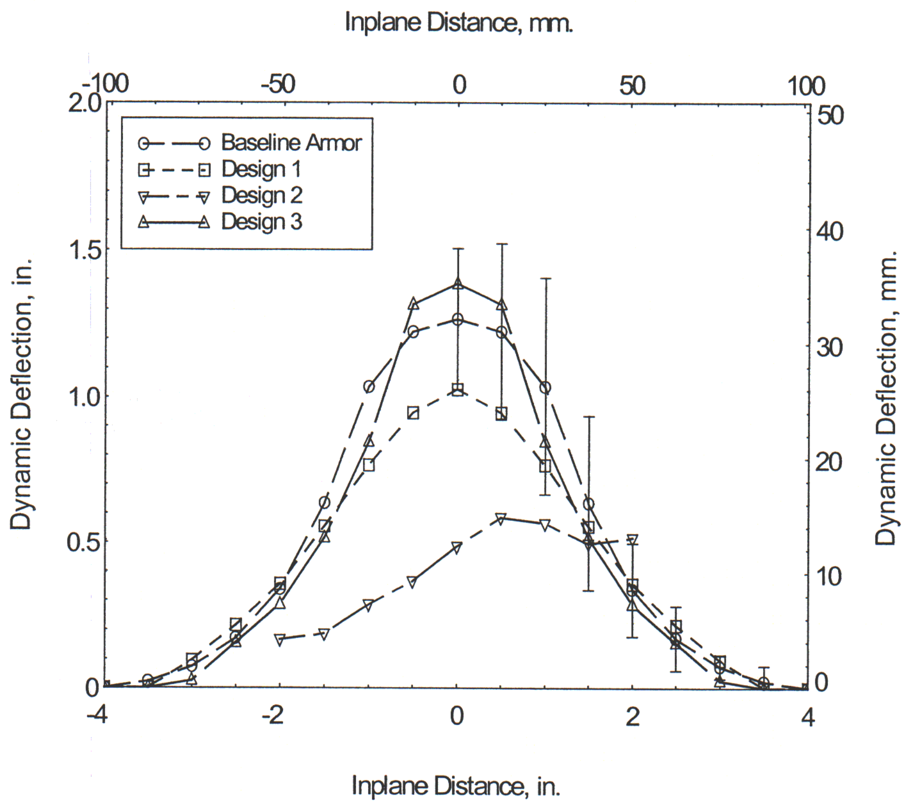

Figure 16. Dynamic deflection of aluminum-foam integral armor.

The armor panels after the ballistic impact is carefully removed from the test fixture such that all the fractured ceramic is contained in the impact cavity other than material ejected during the impact. The impact cavity is then filled with vinyl ester resin to hold the broken ceramic pieces in place. The armor panels are then sectioned, polished, and pictures are taken with a digital camera. These pictures are shown in Figure 16 according to the sequence described in the test matrix and provide us the information on deformation, damage, and relative comparisons between them. The base-line armor shows severe ceramic fracture, cover push-out, penetration through rubber, and the largest volumetric delamination of the backing plate. The load distribution by the fractured ceramic particles on the backing plate during impact is equivalent to one hexagonal tile area. A spring-back effect is observed in all armor panels such that the permanent (static) deformation of the back face is less than 10% of the maximum dynamic deflection.

The overall performance of Design 1 is better than the base line. The volumetric ceramic fracture is less than that of the base line. Most of the ceramic particles are small and medium in size, and almost no pieces are larger than the particles observed in the base line. This pattern of ceramic fracture appears to be superior and is believed to absorb more kinetic energy of the projectile. Deformation of aluminum foam is of inverted bell shape and is localized. The densification of aluminum foam is localized under the projectile head and in a small surrounding area. Since there is no stress-wave transfer to the backing plate before the complete densification, the aluminum foam is acting as a stress wave filter. The deformation pattern of aluminum foam suggests that the load distribution on the backing plate is on a much smaller area than the base line. The volumetric delamination of the backing plate is also less than the base line, possibly due to a significant decrease in premature damage due to stress wave propagation before the arrival of the projectile. It was demonstrated earlier (Figure 15) that the dynamic deflection of Design 1 is less than the base line suggesting that the residual kinetic energy of the projectile pushing the backing plate is less than that of the base line. Design 1 is thus proven to be a better armor solution than the base-line CIA solution with a rubber layer.

The comparison between the Design 2 and the base line is easier if Design 2 is considered the same as the base line with added aluminum-foam backing. The deformation pattern of the cover, ceramic, and rubber layer is similar to the base line. However, the volumetric delamination of the backing plate is less than the base line and is comparable to Design 1. The deformation pattern of the aluminum-foam-backing plate at the composite backing/aluminum-foam interface is a representation of the dynamic deformation of the composite back face. The deformation of aluminum foam is mostly plastic. The dynamic deformation presented in Figure 15 is the deflection of the back face of the aluminum foam, which we can see from Figure 16 as a permanent deformation. The damage in the aluminum-foam-backing plate is distributed over the whole span of the armor plate.

In Design 3, the composite inner layer served the purpose of distributing the load over the aluminum foam. The ceramic fracture is similar to the base line, and this consideration does not yield the benefit of Design 1. Even though the volumetric delamination is least compared to all designs, its dynamic deflection improved only slightly over the base-line CIA.

8. Summary

The unique capability of closed-cell aluminum foam in delaying stress-wave propagation and attenuation is presented through experimental and numerical analyses. It has been found that the dynamic deformation of aluminum foam starts at the impact face and propagates through the thickness till complete densification. The cellular structure makes elastic stress-wave propagation difficult. Effective stress-wave propagation through aluminum foam only occurs after complete densification. If the foam densification is partial, it can act as a stress wave filter. The time required for complete densification appears as a time delay in stress transfer to the next layer (backing plate) and is found to be a linear function of foam thickness. Aluminum foam is also found to reduce the amplitude of the stress pulse transferred to the backing plate. Based on the experimental and numerical stress-wave propagation results, three novel, aluminum-foam, integral armor designs have been evaluated.

Various CIA panels have been ballistically tested under 20-mm FSP impact to assess the associated damage of base-line and aluminum-foam integral armor. The relative study between three different aluminum foam armor designs and their comparison with the base line gives insight into the performance and deformation behavior of this new class of aluminum-foam-based CIA. In comparison to the base line, Design 1 performed the best by providing better ceramic fracture, less cover separation, localized aluminum-foam deformation, less dynamic deflection, and less volumetric delamination of the backing plate. The superior performance of this novel, aluminum-foam, integral armor is a step forward to lighter and more damage-tolerant CIA for the next generation of armored vehicles.

9. References

1. Fink, B. K. "Performance Metrics for Composite Integral Armor." *Journal of Thermoplastic Composite Materials*, vol. 13, pp. 417–431, September 2000.

2. United Defense L. P. *Composite Structure Design Guide*. Composite Armored Vehicle Program, 1997–98.

3. Fink, B. K., and J. W. Gillespie, Jr. "Cost-Effective Manufacturing of Damage Tolerant Integral Armor." ARL-TR-2319, U.S. Army Research Laboratory, Aberdeen Proving Ground, MD, September 2000.

4. Monib, A., J. W. Gillespie, Jr., and B. K. Fink. "Damage Tolerance of Thick-Section Composites Subjected to Ballistic Impact." CCM Report 99–08, University of Delaware, Newark, DE, 1999.

5. Gama, B. A., J. W. Gillespie, Jr., H. Mahfuz, T. A. Bogetti, and B. K. Fink. "Effect of Non-Linear Material Behavior on the Through-Thickness Stress Wave Propagation in Multi-Layer Hybrid Lightweight Armor." Proceedings of International Conference on Computational Engineering and Science, Los Angeles, CA, 21 August 2000.

6. Kenny, L. D. "Mechanical Properties of Particle Stabilized Aluminum Foam." *Mat. Sci. Forum*, vol. 217–222, pp. 1883–1890, 1996.

7. Yu, C. J., and J. Banhart. "Mechanical Properties of Metallic Foams." *Fraunhofer USA Metal Foam Symposium*, pp. 37–48, Stanton, DE, 7–8 October 1997.

8. Deshpande, V. S., and N. A. Fleck. "Isotropic Constitutive Models for Metallic Foams." CUED/C-MICROMECH/TR.9, ISSN 0309-7420, University of Cambridge, November 1998.

9. Deshpande, V. S., and N. A. Fleck. "High Strain Rate Compressive Behavior of Aluminum Alloy Foams." *International Journal of Impact Engineering*, to be published.

10. Yu, C. J., and H. H. Eifert. "Metal Foaming by a Powder Metallurgy Method: Production, Properties, and Applications." *Mat. Res. Innov.*, vol. 2, pp. 181–188, 1998.

11. Yu, C. J., H. H. Eifert, I. W. Hall, R. Franz, and K. Leighton. "Feasibility Study on Deformation Energy Absorption of Metal Foams at High Strain Rates." FC-DE Report No. DAAG55-98-K-0002, November 1998.

12. Yu, C. J., T. D. Claar, H. H. Eifert, I. W. Hall, R. E. Franz, K. T. Leighton, and D. F. Hasson. "Deformation Energy Absorption of Metal Foams at High Strain Rates." *Proc. of Met. Foam*, pp. 347–352, 1999.

13. Franz, R. E., and W. Lawrence. "Stress Measurements in Glass During Shaped-Charge Jet Penetration." BRL-MR-3518, U.S. Army Ballistic Research Laboratory, Aberdeen Proving Ground, MD, 1986.

14. Gama, B. A., T. A. Bogetti, B. K. Fink, H. Mahfuz, and J. W. Gillespie, Jr. "Study of Through-Thickness Wave Propagation in Multi-Layer Hybrid Lightweight Armor." Proceedings of the 13th American Society for Composites Annual Technical Conference, Baltimore, MD, 21–23 September 1998.

15. Meyers, M. A. *Dynamic Behavior of Materials*. New York, NY: John Wiley and Sons, Inc., 1994.

16. Gillio, E. F., J. W. Gillespie, Jr., R. F. Eduljee, S. G. Advani, K. R. Bernetich, and B. K. Fink. "Manufacturing of Composites With the Co-injection Process." Proceedings of the 38th Structural Dynamics and Materiels Conference, American Institute for Astronautics and Aeronautics, Kissimmee, FL, 7–10 April 1997.

NO. OF COPIES	ORGANIZATION
2	DEFENSE TECHNICAL INFORMATION CENTER DTIC OCA 8725 JOHN J KINGMAN RD STE 0944 FT BELVOIR VA 22060-6218
1	HQDA DAMO FDT 400 ARMY PENTAGON WASHINGTON DC 20310-0460
1	OSD OUSD(A&T)/ODDR&E(R) DR R J TREW 3800 DEFENSE PENTAGON WASHINGTON DC 20301-3800
1	COMMANDING GENERAL US ARMY MATERIEL CMD AMCRDA TF 5001 EISENHOWER AVE ALEXANDRIA VA 22333-0001
1	INST FOR ADVNCD TCHNLGY THE UNIV OF TEXAS AT AUSTIN 3925 W BRAKER LN STE 400 AUSTIN TX 78759-5316
1	DARPA SPECIAL PROJECTS OFFICE J CARLINI 3701 N FAIRFAX DR ARLINGTON VA 22203-1714
1	US MILITARY ACADEMY MATH SCI CTR EXCELLENCE MADN MATH MAJ HUBER THAYER HALL WEST POINT NY 10996-1786
1	DIRECTOR US ARMY RESEARCH LAB AMSRL D DR D SMITH 2800 POWDER MILL RD ADELPHI MD 20783-1197

NO. OF COPIES	ORGANIZATION
1	DIRECTOR US ARMY RESEARCH LAB AMSRL CI AI R 2800 POWDER MILL RD ADELPHI MD 20783-1197
3	DIRECTOR US ARMY RESEARCH LAB AMSRL CI LL 2800 POWDER MILL RD ADELPHI MD 20783-1197
3	DIRECTOR US ARMY RESEARCH LAB AMSRL CI AP 2800 POWDER MILL RD ADELPHI MD 20783-1197
	ABERDEEN PROVING GROUND
2	DIR USARL AMSRL CI LP (BLDG 305)

NO. OF COPIES	ORGANIZATION
1	DIRECTOR US ARMY RESEARCH LAB AMSRL CP CA D SNIDER 2800 POWDER MILL RD ADELPHI MD 20783-1145
1	DIRECTOR US ARMY RESEARCH LAB AMSRL OP SD TA 2800 POWDER MILL RD ADELPHI MD 20783-1145
3	DIRECTOR US ARMY RESEARCH LAB AMSRL OP SD TL 2800 POWDER MILL RD ADELPHI MD 20783-1145
1	DIRECTOR US ARMY RESEARCH LAB AMSRL OP SD TP 2800 POWDER MILL RD ADELPHI MD 20783-1145
1	DIRECTOR DA OASARDA SARD SO 103 ARMY PENTAGON WASHINGTON DC 20310-0103
1	DPTY ASST SECY FOR R&T SARD TT THE PENTAGON RM 3EA79 WASHINGTON DC 20301-7100
1	COMMANDER US ARMY MATERIEL CMD AMXMI INT 5001 EISENHOWER AVE ALEXANDRIA VA 22333-0001
4	COMMANDER US ARMY ARDEC AMSTA AR CC G PAYNE J GEHBAUER C BAULIEU H OPAT PICATINNY ARSENAL NJ 07806-5000

NO. OF COPIES	ORGANIZATION
2	COMMANDER US ARMY ARDEC AMSTA AR AE WW E BAKER J PEARSON PICATINNY ARSENAL NJ 07806-5000
1	COMMANDER US ARMY ARDEC AMSTA AR TD C SPINELLI PICATINNY ARSENAL NJ 07806-5000
1	COMMANDER US ARMY ARDEC AMSTA AR FSE PICATINNY ARSENAL NJ 07806-5000
6	COMMANDER US ARMY ARDEC AMSTA AR CCH A W ANDREWS S MUSALLI R CARR M LUCIANO E LOGSDEN T LOUZEIRO PICATINNY ARSENAL NJ 07806-5000
1	COMMANDER US ARMY ARDEC AMSTA AR CCH P J LUTZ PICATINNY ARSENAL NJ 07806-5000
1	COMMANDER US ARMY ARDEC AMSTA AR FSF T C LIVECCHIA PICATINNY ARSENAL NJ 07806-5000
1	COMMANDER US ARMY ARDEC AMSTA ASF PICATINNY ARSENAL NJ 07806-5000

NO. OF COPIES	ORGANIZATION
1	COMMANDER US ARMY ARDEC AMSTA AR QAC T C C PATEL PICATINNY ARSENAL NJ 07806-5000
1	COMMANDER US ARMY ARDEC AMSTA AR M D DEMELLA PICATINNY ARSENAL NJ 07806-5000
3	COMMANDER US ARMY ARDEC AMSTA AR FSA A WARNASH B MACHAK M CHIEFA PICATINNY ARSENAL NJ 07806-5000
2	COMMANDER US ARMY ARDEC AMSTA AR FSP G M SCHIKSNIS D CARLUCCI PICATINNY ARSENAL NJ 07806-5000
1	COMMANDER US ARMY ARDEC AMSTA AR FSP A P KISATSKY PICATINNY ARSENAL NJ 07806-5000
2	COMMANDER US ARMY ARDEC AMSTA AR CCH C H CHANIN S CHICO PICATINNY ARSENAL NJ 07806-5000
1	COMMANDER US ARMY ARDEC AMSTA AR QAC T D RIGOGLIOSO PICATINNY ARSENAL NJ 07806-5000

NO. OF COPIES	ORGANIZATION
1	COMMANDER US ARMY ARDEC AMSTA AR WET T SACHAR BLDG 172 PICATINNY ARSENAL NJ 07806-5000
9	COMMANDER US ARMY ARDEC AMSTA AR CCH B P DONADIA F DONLON P VALENTI C KNUTSON G EUSTICE S PATEL G WAGNECZ R SAYER F CHANG PICATINNY ARSENAL NJ 07806-5000
6	COMMANDER US ARMY ARDEC AMSTA AR CCL F PUZYCKI R MCHUGH D CONWAY E JAROSZEWSKI R SCHLENNER M CLUNE PICATINNY ARSENAL NJ 07806-5000
1	COMMANDER US ARMY ARDEC AMSTA AR SRE D YEE PICATINNY ARSENAL NJ 07806-5000
6	PM SADARM SFAE GCSS SD COL B ELLIS M DEVINE R KOWALSKI W DEMASSI J PRITCHARD S HROWNAK PICATINNY ARSENAL NJ 07806-5000

NO. OF COPIES	ORGANIZATION
1	US ARMY ARDEC INTELLIGENCE SPECIALIST AMSTA AR WEL F M GUERRIERE PICATINNY ARSENAL NJ 07806-5000
2	PEO FIELD ARTILLERY SYS SFAE FAS PM H GOLDMAN T MCWILLIAMS PICATINNY ARSENAL NJ 07806-5000
11	PM TMAS SFAE GSSC TMA R MORRIS C KIMKER D GUZOWICZ E KOPACZ R ROESER R DARCY R MCDANOLDS L D ULISSE C ROLLER J MCGREEN B PATTER PICATINNY ARSENAL NJ 07806-5000
1	COMMANDER US ARMY ARDEC AMSTA AR WEA J BRESCIA PICATINNY ARSENAL NJ 07806-5000
1	COMMANDER US ARMY ARDEC PRODUCTION BASE MODERN ACTY AMSMC PBM K PICATINNY ARSENAL NJ 07806-5000
1	COMMANDER US ARMY TACOM PM ABRAMS SFAE ASM AB 6501 ELEVEN MILE RD WARREN MI 48397-5000

NO. OF COPIES	ORGANIZATION
1	COMMANDER US ARMY TACOM AMSTA SF WARREN MI 48397-5000
3	COMMANDER US ARMY TACOM PM TACTICAL VEHICLES SFAE TVL SFAE TVM SFAE TVH 6501 ELEVEN MILE RD WARREN MI 48397-5000
1	COMMANDER US ARMY TACOM PM BFVS SFAE ASM BV 6501 ELEVEN MILE RD WARREN MI 48397-5000
1	COMMANDER US ARMY TACOM PM AFAS SFAE ASM AF 6501 ELEVEN MILE RD WARREN MI 48397-5000
1	COMMANDER US ARMY TACOM PM RDT&E SFAE GCSS W AB J GODELL 6501 ELEVEN MILE RD WARREN MI 48397-5000
2	COMMANDER US ARMY TACOM PM SURV SYS SFAE ASM SS T DEAN SFAE GCSS W GSI M D COCHRAN 6501 ELEVEN MILE RD WARREN MI 48397-5000
1	US ARMY CERL R LAMPO 2902 NEWMARK DR CHAMPAIGN IL 61822

NO. OF COPIES	ORGANIZATION
1	COMMANDER US ARMY TACOM PM SURVIVABLE SYSTEMS SFAE GCSS W GSI H M RYZYI 6501 ELEVEN MILE RD WARREN MI 48397-5000
1	COMMANDER US ARMY TACOM PM BFV SFAE GCSS W BV S DAVIS 6501 ELEVEN MILE RD WARREN MI 48397-5000
1	COMMANDER US ARMY TACOM PM LIGHT TACTICAL VHCLS AMSTA TR S A J MILLS MS 209 6501 ELEVEN MILE RD WARREN MI 48397-5000
1	COMMANDER US ARMY TACOM CHIEF ABRAMS TESTING SFAE GCSS W AB QT T KRASKIEWICZ 6501 ELEVEN MILE RD WARREN MI 48397-5000
1	COMMANDER WATERVLIET ARSENAL SMCWV QAE Q B VANINA BLDG 44 WATERVLIET NY 12189-4050
1	COMMANDER WATERVLIET ARSENAL SMCWV SPM T MCCLOSKEY BLDG 253 WATERVLIET NY 12189-4050
2	TSM ABRAMS ATZK TS S JABURG W MEINSHAUSEN FT KNOX KY 40121

NO. OF COPIES	ORGANIZATION
15	COMMANDER US ARMY TACOM AMSTA TR R J CHAPIN R MCCLELLAND D THOMAS J BENNETT D HANSEN AMSTA JSK S GOODMAN J FLORENCE K IYER D TEMPLETON A SCHUMACHER AMSTA TR D D OSTBERG L HINOJOSA B RAJU AMSTA CS SF H HUTCHINSON F SCHWARZ WARREN MI 48397-5000
3	ARMOR SCHOOL ATZK TD R BAUEN J BERG A POMEY FT KNOX KY 40121
11	BENET LABORATORIES AMSTA AR CCB R FISCELLA G D ANDREA E KATHE M SCAVULO G SPENCER P WHEELER K MINER J VASILAKIS G FRIAR R HASENBEIN AMSTA CCB R S SOPOK WATERVLIET NY 12189-4050
2	HQ IOC TANK AMMUNITION TEAM AMSIO SMT R CRAWFORD W HARRIS ROCK ISLAND IL 61299-6000

NO. OF COPIES	ORGANIZATION
2	DAVID TAYLOR RESEARCH CTR R ROCKWELL W PHYILLAIER BETHESDA MD 20054-5000
2	COMMANDER US ARMY AMCOM AVIATION APPLIED TECH DIR J SCHUCK FT EUSTIS VA 23604-5577
1	DIRECTOR US ARMY AMCOM SFAE AV RAM TV D CALDWELL BLDG 5300 REDSTONE ARSENAL AL 35898
2	US ARMY CORPS OF ENGINEERS CERD C T LIU CEW ET T TAN 20 MASS AVE NW WASHINGTON DC 20314
1	US ARMY COLD REGIONS RSCH & ENGRNG LAB P DUTTA 72 LYME RD HANOVER NH 03755
1	SYSTEM MANAGER ABRAMS ATZK TS LTC J H NUNN BLDG 1002 RM 110 FT KNOX KY 40121
1	USA SBCCOM PM SOLDIER SPT AMSSB PM RSS A J CONNORS KANSAS ST NATICK MA 01760-5057
3	BALLISTICS TEAM AMSSB RIP PHIL CUNNIFF JOHN SONG WALTER ZUKAS KANSAS ST NATICK MA 01760-5057

NO. OF COPIES	ORGANIZATION
2	MATERIAL SCIENCE TEAM AMSSB RSS JEAN HERBERT MICHAEL SENNETT KANSAS ST NATICK MA 01760-5057
2	OFC OF NAVAL RESEARCH D SIEGEL CODE 351 J KELLY 800 N QUINCY ST ARLINGTON VA 22217-5660
1	NAVAL SURFACE WARFARE CTR DAHLGREN DIV CODE G06 DAHLGREN VA 22448
1	NAVAL SURFACE WARFARE CTR TECH LIBRARY CODE 323 17320 DAHLGREN RD DAHLGREN VA 22448
1	NAVAL SURFACE WARFARE CTR CRANE DIVISION M JOHNSON CODE 20H4 LOUISVILLE KY 40214-5245
8	DIRECTOR US ARMY NATIONAL GROUND INTELLIGENCE CTR D LEITER M HOLTUS M WOLFE S MINGLEDORF J GASTON W GSTATTENBAUER R WARNER J CRIDER 220 SEVENTH ST NE CHARLOTTESVILLE VA 22091
3	NAVAL RESEARCH LAB I WOLOCK CODE 6383 R BADALIANCE CODE 6304 L GAUSE WASHINGTON DC 20375
2	NAVAL SURFACE WARFARE CTR U SORATHIA C WILLIAMS CD 6551 9500 MACARTHUR BLVD WEST BETHESDA MD 20817

NO. OF COPIES	ORGANIZATION
6	US ARMY SBCCOM SOLDIER SYSTEMS CENTER BALLISTICS TEAM J WARD MARINE CORPS TEAM J MACKIEWICZ BUS AREA ADVOCACY TEAM W HASKELL SSCNC WST W NYKVIST T MERRILL S BEAUDOIN KANSAS ST NATICK MA 01760-5019
9	US ARMY RESEARCH OFC A CROWSON J CHANDRA H EVERETT J PRATER R SINGLETON G ANDERSON D STEPP D KISEROW J CHANG PO BOX 12211 RESEARCH TRIANGLE PARK NC 27709-2211
8	NAVAL SURFACE WARFARE CTR J FRANCIS CODE G30 D WILSON CODE G32 R D COOPER CODE G32 J FRAYSSE CODE G33 E ROWE CODE G33 T DURAN CODE G33 L DE SIMONE CODE G33 R HUBBARD CODE G33 DAHLGREN VA 22448
2	COMMANDER NAVAL SURFACE WARFARE CTR CARDEROCK DIVISION R PETERSON CODE 2020 M CRITCHFIELD CODE 1730 BETHESDA MD 20084
1	NAVAL SEA SYSTEMS CMD D LIESE 2531 JEFFERSON DAVIS HWY ARLINGTON VA 22242-5160

NO. OF COPIES	ORGANIZATION
1	NAVAL SURFACE WARFARE CTR M LACY CODE B02 17320 DAHLGREN RD DAHLGREN VA 22448
2	NAVAL SURFACE WARFARE CTR CARDEROCK DIVISION R CRANE CODE 2802 C WILLIAMS CODE 6553 3A LEGGETT CIR BETHESDA MD 20054-5000
1	EXPEDITIONARY WARFARE DIV N85 F SHOUP 2000 NAVY PENTAGON WASHINGTON DC 20350-2000
1	AFRL MLBC 2941 P ST RM 136 WRIGHT PATTERSON AFB OH 45433-7750
1	AFRL MLSS R THOMSON 2179 12TH ST RM 122 WRIGHT PATTERSON AFB OH 45433-7718
2	AFRL F ABRAMS J BROWN BLDG 653 2977 P ST STE 6 WRIGHT PATTERSON AFB OH 45433-7739
1	WATERWAYS EXPERIMENT D SCOTT 3909 HALLS FERRY RD SC C VICKSBURG MS 39180
5	DIRECTOR LLNL R CHRISTENSEN S DETERESA F MAGNESS M FINGER MS 313 M MURPHY L 282 PO BOX 808 LIVERMORE CA 94550

NO. OF COPIES	ORGANIZATION
1	AFRL MLS OL L COULTER 7278 4TH ST BLDG 100 BAY D HILL AFB UT 84056-5205
1	OSD JOINT CCD TEST FORCE OSD JCCD R WILLIAMS 3909 HALLS FERRY RD VICKSBURG MS 29180-6199
1	DEFENSE NUCLEAR AGENCY INNOVATIVE CONCEPTS DIV 6801 TELEGRAPH RD ALEXANDRIA VA 22310-3398
3	DARPA M VANFOSSEN S WAX L CHRISTODOULOU 3701 N FAIRFAX DR ARLINGTON VA 22203-1714
2	FAA TECH CENTER P SHYPRYKEVICH AAR 431 ATLANTIC CITY NJ 08405
2	SERDP PROGRAM OFC PM P2 C PELLERIN B SMITH 901 N STUART ST STE 303 ARLINGTON VA 22203
1	FAA MIL HDBK 17 CHAIR L ILCEWICZ 1601 LIND AVE SW ANM 115N RESTON VA 98055
1	US DEPT OF ENERGY OFC OF ENVIRONMENTAL MANAGEMENT P RITZCOVAN 19901 GERMANTOWN RD GERMANTOWN MD 20874-1928

NO. OF COPIES	ORGANIZATION
1	DIRECTOR LLNL F ADDESSIO MS B216 PO BOX 1633 LOS ALAMOS NM 87545
1	OAK RIDGE NATIONAL LABORATORY R M DAVIS PO BOX 2008 OAK RIDGE TN 37831-6195
3	DIRECTOR SANDIA NATIONAL LABS APPLIED MECHANICS DEPT MS 9042 J HANDROCK Y R KAN J LAUFFER PO BOX 969 LIVERMORE CA 94551-0969
1	OAK RIDGE NATIONAL LABORATORY C EBERLE MS 8048 PO BOX 2008 OAK RIDGE TN 37831
1	OAK RIDGE NATIONAL LABORATORY C D WARREN MS 8039 PO BOX 2008 OAK RIDGE TN 37831
7	NIST R PARNAS J DUNKERS M VANLANDINGHAM MS 8621 J CHIN MS 8621 D HUNSTON MS 8543 J MARTIN MS 8621 D DUTHINH MS 8611 100 BUREAU DR GAITHERSBURG MD 20899
1	HYDROGEOLOGIC INC SERDP ESTCP SPT OFC S WALSH 1155 HERNDON PKWY STE 900 HERNDON VA 20170

NO. OF COPIES	ORGANIZATION
3	NASA LANGLEY RSCH CTR AMSRL VS W ELBER MS 266 F BARTLETT JR MS 266 G FARLEY MS 266 HAMPTON VA 23681-0001
1	NASA LANGLEY RSCH CTR T GATES MS 188E HAMPTON VA 23661-3400
1	FHWA E MUNLEY 6300 GEORGETOWN PIKE MCLEAN VA 22101
4	CYTEC FIBERITE R DUNNE D KOHLI M GILLIO R MAYHEW 1300 REVOLUTION ST HAVRE DE GRACE MD 21078
1	USDOT FEDERAL RAILRD M FATEH RDV 31 WASHINGTON DC 20590
1	CENTRAL INTLLGNC AGNCY OTI WDAG GT W L WALTMAN PO BOX 1925 WASHINGTON DC 20505
1	MARINE CORPS INTLLGNC ACTVTY D KOSITZKE 3300 RUSSELL RD STE 250 QUANTICO VA 22134-5011
1	DIRECTOR NATIONAL GRND INTLLGNC CTR IANG TMT 220 SEVENTH ST NE CHARLOTTESVILLE VA 22902-5396
1	SIOUX MFG B KRIEL PO BOX 400 FT TOTTEN ND 58335

NO. OF COPIES	ORGANIZATION
1	DIRECTOR DEFENSE INTLLGNC AGNCY TA 5 K CRELLING WASHINGTON DC 20310
1	ADVANCED GLASS FIBER YARNS T COLLINS 281 SPRING RUN LANE STE A DOWNINGTON PA 19335
1	COMPOSITE MATERIALS INC D SHORTT 19105 63 AVE NE PO BOX 25 ARLINGTON WA 98223
1	JPS GLASS L CARTER PO BOX 260 SLATER RD SLATER SC 29683
1	COMPOSITE MATERIALS INC R HOLLAND 11 JEWEL CT ORINDA CA 94563
1	COMPOSITE MATERIALS INC C RILEY 14530 S ANSON AVE SANTA FE SPRINGS CA 90670
2	COMPOSIX D BLAKE L DIXON 120 O NEILL DR HEBRUN OH 43025
2	SIMULA J COLTMAN R HUYETT 10016 S 51ST ST PHOENIX AZ 85044
2	PROTECTION MATERIALS INC M MILLER F CRILLEY 14000 NW 58 CT MIAMI LAKES FL 33014

NO. OF COPIES	ORGANIZATION
3	FOSTER MILLER J J GASSNER M ROYLANCE W ZUKAS 195 BEAR HILL RD WALTHAM MA 02354-1196
1	ROM DEVELOPMENT CORP R O MEARA 136 SWINEBURNE ROW BRICK MARKET PLACE NEWPORT RI 02840
2	TEXTRON SYSTEMS T FOLTZ M TREASURE 201 LOWELL ST WILMINGTON MA 08870-2941
1	GLCC INC J RAY 103 TRADE ZONE DR STE 26C WEST COLUMBIA SC 29170
1	O GARA HESS & EISENHARDT M GILLESPIE 9113 LESAINT DR FAIRFIELD OH 45014
2	MILLIKEN RSCH CORP H KUHN M MACLEOD PO BOX 1926 SPARTANBURG SC 29303
1	CONNEAUGHT INDUSTRIES INC J SANTOS PO BOX 1425 COVENTRY RI 02816
2	BATTELLE NATICK OPNS J CONNORS B HALPIN 209 W CENTRAL ST STE 302 NATICK MA 01760
1	ARMTEC DEFENSE PRODUCTS S DYER 85 901 AVE 53 PO BOX 848 COACHELLA CA 92236

NO. OF COPIES	ORGANIZATION
3	PACIFIC NORTHWEST LAB M SMITH G VAN ARSDALE R SHIPPELL PO BOX 999 RICHLAND WA 99352
8	ALLIANT TECHSYSTEMS INC C CANDLAND MN11 2830 C AAKHUS MN11 2830 B SEE MN11 2439 N VLAHAKUS MN11 2145 R DOHRN MN11 2830 S HAGLUND MN11 2439 M HISSONG MN11 2830 D KAMDAR MN11 2830 600 SECOND ST NE HOPKINS MN 55343-8367
2	AMOCO PERFORMANCE PRODUCTS M MICHNO JR J BANISAUKAS 4500 MCGINNIS FERRY RD ALPHARETTA GA 30202-3944
1	SAIC M PALMER 1410 SPRING HILL RD STE 400 MS SH4 5 MCLEAN VA 22102
1	SAIC G CHRYSSOMALLIS 3800 W 80TH ST STE 1090 BLOOMINGTON MN 55431
1	AAI CORPORATION T G STASTNY PO BOX 126 HUNT VALLEY MD 21030-0126
1	APPLIED COMPOSITES W GRISCH 333 NORTH SIXTH ST ST CHARLES IL 60174
1	CUSTOM ANALYTICAL ENG SYS INC A ALEXANDER 13000 TENSOR LANE NE FLINTSTONE MD 21530

NO. OF COPIES	ORGANIZATION
3	ALLIANT TECHSYSTEMS INC J CONDON E LYNAM J GERHARD WV01 16 STATE RT 956 PO BOX 210 ROCKET CENTER WV 26726-0210
1	OFC DEPUTY UNDER SEC DEFNS JAMES THOMPSON 1745 JEFFERSON DAVIS HWY CRYSTAL SQ 4 STE 501 ARLINGTON VA 22202
1	PROJECTILE TECHNOLOGY INC 515 GILES ST HAVRE DE GRACE MD 21078
5	AEROJET GEN CORP D PILLASCH T COULTER C FLYNN D RUBAREZUL M GREINER 1100 WEST HOLLYVALE ST AZUSA CA 91702-0296
3	HEXCEL INC R BOE PO BOX 18748 SALT LAKE CITY UT 84118
1	HERCULES INC HERCULES PLAZA WILMINGTON DE 19894
1	BRIGS COMPANY J BACKOFEN 2668 PETERBOROUGH ST HERNDON VA 22071-2443
1	ZERNOW TECHNICAL SERVICES L ZERNOW 425 W BONITA AVE STE 208 SAN DIMAS CA 91773
1	OLIN CORPORATION L WHITMORE 10101 NINTH ST NORTH ST PETERSBURG FL 33702

NO. OF COPIES	ORGANIZATION
2	OLIN CORPORATION FLINCHBAUGH DIV E STEINER B STEWART PO BOX 127 RED LION PA 17356
1	GKN AEROSPACE D OLDS 15 STERLING DR WALLINGFORD CT 06492
5	SIKORSKY AIRCRAFT G JACARUSO T CARSTENSAN B KAY S GARBO MS S330A J ADELMANN 6900 MAIN ST PO BOX 9729 STRATFORD CT 06497-9729
1	PRATT & WHITNEY C WATSON 400 MAIN ST MS 114 37 EAST HARTFORD CT 06108
1	AEROSPACE CORP G HAWKINS M4 945 2350 E EL SEGUNDO BLVD EL SEGUNDO CA 90245
2	CYTEC FIBERITE M LIN W WEB 1440 N KRAEMER BLVD ANAHEIM CA 92806
1	HEXCEL T BITZER 11711 DUBLIN BLVD DUBLIN CA 94568
1	BOEING R BOHLMANN PO BOX 516 MC 5021322 ST LOUIS MO 63166-0516
1	UDLP G THOMAS PO BOX 58123 SANTA CLARA CA 95052

NO. OF COPIES	ORGANIZATION
2	UDLP R BARRETT MAIL DROP M53 V HORVATICH MAIL DROP M53 328 W BROKAW RD SANTA CLARA CA 95052-0359
3	UDLP GROUND SYSTEMS DIVISION M PEDRAZZI MAIL DROP N09 A LEE MAIL DROP N11 M MACLEAN MAIL DROP N06 1205 COLEMAN AVE SANTA CLARA CA 95052
4	UDLP R BRYNSVOLD P JANKE MS 170 4800 EAST RIVER RD MINNEAPOLIS MN 55421-1498
1	UDLP D MARTIN PO BOX 359 SANTA CLARA CA 95052
2	BOEING DFNSE & SPACE GP W HAMMOND S 4X55 J RUSSELL S 4X55 PO BOX 3707 SEATTLE WA 98124-2207
2	BOEING ROTORCRAFT P MINGURT P HANDEL 800 B PUTNAM BLVD WALLINGFORD PA 19086
1	BOEING DOUGLAS PRODUCTS DIV L J HART SMITH 3855 LAKEWOOD BLVD D800 0019 LONG BEACH CA 90846-0001
1	LOCKHEED MARTIN S REEVE 8650 COBB DR D 73 62 MZ 0648 MARIETTA GA 30063-0648

NO. OF COPIES	ORGANIZATION
1	LOCKHEED MARTIN SKUNK WORKS D FORTNEY 1011 LOCKHEED WAY PALMDALE CA 93599-2502
1	LOCKHEED MARTIN R FIELDS 1195 IRWIN CT WINTER SPRINGS FL 32708
1	MATERIALS SCIENCES CORP B W ROSEN 500 OFC CENTER DR STE 250 FT WASHINGTON PA 19034
1	NORTHRUP GRUMMAN CORP ELECTRONIC SENSORS & SYSTEMS DIV E SCHOCH MS V 16 1745A W NURSERY RD LINTHICUM MD 21090
2	NORTHROP GRUMMAN ENVIRONMENTAL PROGRAMS R OSTERMAN A YEN 8900 E WASHINGTON BLVD PICO RIVERA CA 90660
1	GDLS DIVISION D BARTLE PO BOX 1901 WARREN MI 48090
2	GDLS D REES M PASIK PO BOX 2074 WARREN MI 48090-2074
1	GDLS MUSKEGON OPERATIONS W SOMMERS JR 76 GETTY ST MUSKEGON MI 49442

NO. OF COPIES	ORGANIZATION
1	GENERAL DYNAMICS AMPHIBIOUS SYS SURVIVABILITY LEAD G WALKER 991 ANNAPOLIS WAY WOODBRIDGE VA 22191
6	INST FOR ADVANCED TECH H FAIR I MCNAB P SULLIVAN S BLESS W REINECKE C PERSAD 3925 W BRAKER LN STE 400 AUSTIN TX 78759-5316
2	CIVIL ENGR RSCH FOUNDATION PRESIDENT H BERNSTEIN R BELLE 1015 15TH ST NW STE 600 WASHINGTON DC 20005
1	ARROW TECH ASSO 1233 SHELBURNE RD STE D8 SOUTH BURLINGTON VT 05403-7700
1	R EICHELBERGER CONSULTANT 409 W CATHERINE ST BEL AIR MD 21014-3613
1	UCLA MANE DEPT ENGR IV H T HAHN LOS ANGELES CA 90024-1597
2	UNIV OF DAYTON RESEARCH INST R Y KIM A K ROY 300 COLLEGE PARK AVE DAYTON OH 45469-0168
1	MIT P LAGACE 77 MASS AVE CAMBRIDGE MA 01887

NO. OF COPIES	ORGANIZATION
1	IIT RESEARCH CENTER D ROSE 201 MILL ST ROME NY 13440-6916
1	GA TECH RSCH INST GA INST OF TCHNLGY P FRIEDERICH ATLANTA GA 30392
1	MICHIGAN ST UNIV MSM DEPT R AVERILL 3515 EB EAST LANSING MI 48824-1226
1	UNIV OF KENTUCKY L PENN 763 ANDERSON HALL LEXINGTON KY 40506-0046
1	UNIV OF WYOMING D ADAMS PO BOX 3295 LARAMIE WY 82071
2	PENN STATE UNIV R MCNITT C BAKIS 212 EARTH ENGR SCIENCES BLDG UNIVERSITY PARK PA 16802
1	PENN STATE UNIV R S ENGEL 245 HAMMOND BLDG UNIVERSITY PARK PA 16801
1	PURDUE UNIV SCHOOL OF AERO & ASTRO C T SUN W LAFAYETTE IN 47907-1282
1	STANFORD UNIV DEPT OF AERONAUTICS & AEROBALLISTICS S TSAI DURANT BLDG STANFORD CA 94305

NO. OF COPIES	ORGANIZATION
1	UNIV OF DAYTON J M WHITNEY COLLEGE PARK AVE DAYTON OH 45469-0240
7	UNIV OF DELAWARE CTR FOR COMPOSITE MTRLS J GILLESPIE M SANTARE G PALMESE S YARLAGADDA S ADVANI D HEIDER D KUKICH 201 SPENCER LABORATORY NEWARK DE 19716
1	DEPT OF MATERIALS SCIENCE & ENGINEERING UNIVERSITY OF ILLINOIS AT URBANA CHAMPAIGN J ECONOMY 1304 WEST GREEN ST 115B URBANA IL 61801
1	NORTH CAROLINA STATE UNIV CIVIL ENGINEERING DEPT W RASDORF PO BOX 7908 RALEIGH NC 27696-7908
1	UNIV OF MARYLAND DEPT OF AEROSPACE ENGNRNG A J VIZZINI COLLEGE PARK MD 20742
3	UNIV OF TEXAS AT AUSTIN CTR FOR ELECTROMECHANICS J PRICE A WALLS J KITZMILLER 10100 BURNET RD AUSTIN TX 78758-4497
3	VA POLYTECHNICAL INST & STATE UNIV DEPT OF ESM M W HYER K REIFSNIDER R JONES BLACKSBURG VA 24061-0219

NO. OF COPIES	ORGANIZATION
1	DREXEL UNIV A S D WANG 32ND & CHESTNUT ST PHILADELPHIA PA 19104
1	SOUTHWEST RSCH INST ENGR & MATL SCIENCES DIV J RIEGEL 6220 CULEBRA RD PO DRAWER 28510 SAN ANTONIO TX 78228-0510
	ABERDEEN PROVING GROUND
1	US ARMY MATERIEL SYSTEMS ANALYSIS ACTIVITY P DIETZ 392 HOPKINS RD AMXSY TD APG MD 21005-5071
1	DIRECTOR US ARMY RESEARCH LAB AMSRL OP AP L APG MD 21005-5066
105	DIR USARL AMSRL CI AMSRL CI H W STUREK AMSRL CI S A MARK AMSRL CS IO FI M ADAMSON AMSRL SL B J SMITH AMSRL SL BA AMSRL SL BL D BELY R HENRY AMSRL SL BG AMSRL SL I AMSRL WM E SCHMIDT AMSRL WM B A HORST AMSRL WM BA F BRANDON

NO. OF COPIES	ORGANIZATION
	ABERDEEN PROVING GROUND (CONT)
	AMSRL WM BC P PLOSTINS D LYON J NEWILL S WILKERSON A ZIELINSKI
	AMSRL WM BD B FORCH R FIFER R PESCE RODRIGUEZ B RICE
	AMSRL WM BE C LEVERITT D KOOKER
	AMSRL WM BR C SHOEMAKER J BORNSTEIN
	AMSRL WM M D VIECHNICKI G HAGNAUER J MCCAULEY B TANNER
	AMSRL WM MA R SHUFORD P TOUCHET N BECK TAN
	AMSRL WM MA D FLANAGAN L GHIORSE D HARRIS S MCKNIGHT P MOY P PATTERSON G RODRIGUEZ A TEETS R YIN
	AMSRL WM MB B FINK J BENDER T BOGETTI R BOSSOLI L BURTON K BOYD S CORNELISON P DEHMER R DOOLEY W DRYSDALE G GAZONAS S GHIORSE D GRANVILLE

NO. OF COPIES	ORGANIZATION
	ABERDEEN PROVING GROUND (CONT)
	AMSRL WM MB D HOPKINS C HOPPEL D HENRY R KASTE M KLUSEWITZ M LEADORE R LIEB E RIGAS J SANDS D SPAGNUOLO W SPURGEON J TZENG E WETZEL A FRYDMAN
	AMRSL WM MC J BEATTY E CHIN J MONTGOMERY A WERECZCAK J LASALVIA J WELLS
	AMSRL WM MD W ROY S WALSH
	AMSRL WM T B BURNS
	AMSRL WM TA W GILLICH T HAVEL J RUNYEON M BURKINS E HORWATH B GOOCH W BRUCHEY
	AMSRL WM TC R COATES
	AMSRL WM TD A DAS GUPTA T HADUCH T MOYNIHAN F GREGORY A RAJENDRAN M RAFTENBERG M BOTELER T WEERASOORIYA D DANDEKAR A DIETRICH

NO. OF
COPIES ORGANIZATION

ABERDEEN PROVING GROUND (CONT)

AMSRL WM TE
A NIILER
J POWELL
AMSRL SS SD
H WALLACE
AMSRL SS SE R
R CHASE
AMSRL SS SE DS
R REYZER
R ATKINSON
AMSRL SE L
R WEINRAUB
J DESMOND
D WOODBURY

NO. OF COPIES	ORGANIZATION
1	LTD R MARTIN MERL TAMWORTH RD HERTFORD SG13 7DG UK
1	SMC SCOTLAND P W LAY DERA ROSYTH ROSYTH ROYAL DOCKYARD DUNFERMLINE FIFE KY 11 2XR UK
1	CIVIL AVIATION ADMINSTRATION T GOTTESMAN PO BOX 8 BEN GURION INTERNL AIRPORT LOD 70150 ISRAEL
1	AEROSPATIALE S ANDRE A BTE CC RTE MD132 316 ROUTE DE BAYONNE TOULOUSE 31060 FRANCE
3	DRA FORT HALSTEAD P N JONES M HINTON SEVEN OAKS KENT TN 147BP UK
1	DEFENSE RESEARCH ESTAB VALCARTIER F LESAGE COURCELETTE QUEBEC COA IRO CANADA
1	SWISS FEDERAL ARMAMENTS WKS W LANZ ALLMENDSTRASSE 86 3602 THUN SWITZERLAND
1	DYNAMEC RESEARCH AB AKE PERSSON BOX 201 SE 151 23 SODERTALJE SWEDEN

NO. OF COPIES	ORGANIZATION
1	ISRAEL INST OF TECHNOLOGY S BODNER FACULTY OF MECHANICAL ENGR HAIFA 3200 ISRAEL
1	DSTO MATERIALS RESEARCH LAB NAVAL PLATFORM VULNERABILITY SHIP STRUCTURES & MTRLS DIV N BURMAN PO BOX 50 ASCOT VALE VICTORIA AUSTRALIA 3032
1	ECOLE ROYAL MILITAIRE E CELENS AVE DE LA RENAISSANCE 30 1040 BRUXELLE BELGIQUE
1	DEF RES ESTABLISHMENT VALCARTIER A DUPUIS 2459 BOULEVARD PIE XI NORTH VALCARTIER QUEBEC CANADA PO BOX 8800 COURCELETTE GOA IRO QUEBEC CANADA
1	INSTITUT FRANCO ALLEMAND DE RECHERCHES DE SAINT LOUIS DE M GIRAUD 5 RUE DU GENERAL CASSAGNOU BOITE POSTALE 34 F 68301 SAINT LOUIS CEDEX FRANCE
1	ECOLE POLYTECH J MANSON DMX LTC CH 1015 LAUSANNE SWITZERLAND

NO. OF COPIES	ORGANIZATION
1	TNO PRINS MAURITS LABORATORY R IJSSELSTEIN LANGE KLEIWEG 137 PO BOX 45 2280 AA RIJSWIJK THE NETHERLANDS
2	FOA NATL DEFENSE RESEARCH ESTAB DIR DEPT OF WEAPONS & PROTECTION B JANZON R HOLMLIN S 172 90 STOCKHOLM SWEDEN
2	DEFENSE TECH & PROC AGENCY GROUND I CREWTHER GENERAL HERZOG HAUS 3602 THUN SWITZERLAND
1	MINISTRY OF DEFENCE RAFAEL ARMAMENT DEVELOPMENT AUTH M MAYSELESS PO BOX 2250 HAIFA 31021 ISRAEL
1	TNO DEFENSE RESEARCH I H PASMAN POSTBUS 6006 2600 JA DELFT THE NETHERLANDS
1	B HIRSCH TACHKEMONY ST 6 NETAMUA 42611 ISRAEL
1	DEUTSCHE AEROSPACE AG DYNAMICS SYSTEMS M HELD PO BOX 1340 D 86523 SCHROBENHAUSEN GERMANY

REPORT DOCUMENTATION PAGE

Form Approved
OMB No. 0704-0188

Public reporting burden for this collection of information is estimated to average 1 hour per response, including the time for reviewing instructions, searching existing data sources, gathering and maintaining the data needed, and completing and reviewing the collection of information. Send comments regarding this burden estimate or any other aspect of this collection of information, including suggestions for reducing this burden, to Washington Headquarters Services, Directorate for Information Operations and Reports, 1215 Jefferson Davis Highway, Suite 1204, Arlington, VA 22202-4302, and to the Office of Management and Budget, Paperwork Reduction Project(0704-0188), Washington, DC 20503.

1. AGENCY USE ONLY *(Leave blank)*

2. REPORT DATE
May 2001

3. REPORT TYPE AND DATES COVERED
October 1999 - May 2000

4. TITLE AND SUBTITLE
Application of Aluminum Foam for Stress-Wave Management in Lightweight Composite Integral Armor

5. FUNDING NUMBERS
AH42

6. AUTHOR(S)
Bruce K. Fink, Travis A. Bogetti, Bazle Gama,* John W. Gillespie, Jr.,*
Chin-Jye Yu,† T. Dennis Claar,† and Harald H. Eifert†

7. PERFORMING ORGANIZATION NAME(S) AND ADDRESS(ES)
U.S. Army Research Laboratory
ATTN: AMSRL-WM-MB
Aberdeen Proving Ground, MD 21005-5069

8. PERFORMING ORGANIZATION REPORT NUMBER
ARL-TR-2471

9. SPONSORING/MONITORING AGENCY NAMES(S) AND ADDRESS(ES)

10. SPONSORING/MONITORING AGENCY REPORT NUMBER

11. SUPPLEMENTARY NOTES
* University of Delaware, Newark, DE 19716
† Fraunhofer USA, Plymouth, MI 48170

12a. DISTRIBUTION/AVAILABILITY STATEMENT
Approved for public release; distribution is unlimited.

12b. DISTRIBUTION CODE

13. ABSTRACT *(Maximum 200 words)*

Closed-cell aluminum foam offers a unique combination of properties such as low density, high stiffness, strength, and energy absorption that can be tailored through design of the microstructure. During ballistic impact, the foam exhibits significant nonlinear deformation and stress-wave attenuation. Composite structural armor panels containing closed-cell aluminum foam are impacted with 20-mm fragment-simulating projectiles (FSP). One-dimensional plane strain finite element analysis (FEA) of stress-wave propagation is performed to understand the dynamic response and deformation mechanisms. The FEA results correlate well with the experimental observation that aluminum foam can delay and attenuate stress waves. It is identified that the aluminum foam transmits an insignificant amount of stress pulse before complete densification. The ballistic performance of aluminum foam-based composite integral armor is compared with the base-line integral armor of equivalent areal density by impacting panels with 20-mm FSP. A comparative damage study reveals that the aluminum-foam armor has better and finer ceramic fracture and less volumetric delamination of the composite backing plate as compared to the base line. The aluminum-foam armors also showed less dynamic deflection of the backing plate than the base line. These attributes of the aluminum foam in integral armor system add a new dimension in the design of lightweight armor for the future armored vehicles.

14. SUBJECT TERMS
composite material, integral armor, resin transfer molding, aluminum foam, ballistic

15. NUMBER OF PAGES
48

16. PRICE CODE

17. SECURITY CLASSIFICATION OF REPORT	18. SECURITY CLASSIFICATION OF THIS PAGE	19. SECURITY CLASSIFICATION OF ABSTRACT	20. LIMITATION OF ABSTRACT
UNCLASSIFIED	UNCLASSIFIED	UNCLASSIFIED	UL

NSN 7540-01-280-5500

Standard Form 298 (Rev. 2-89)
Prescribed by ANSI Std. 239-18 298-102

INTENTIONALLY LEFT BLANK.

USER EVALUATION SHEET/CHANGE OF ADDRESS

This Laboratory undertakes a continuing effort to improve the quality of the reports it publishes. Your comments/answers to the items/questions below will aid us in our efforts.

1. ARL Report Number/Author ARL-TR-2471 (Fink) ____________ Date of Report May 2001 ________

2. Date Report Received ________________________________

3. Does this report satisfy a need? (Comment on purpose, related project, or other area of interest for which the report will be used.) ________________________________

____

4. Specifically, how is the report being used? (Information source, design data, procedure, source of ideas, etc.) ________

____

____

5. Has the information in this report led to any quantitative savings as far as man-hours or dollars saved, operating costs avoided, or efficiencies achieved, etc? If so, please elaborate. ________________________________

____

____

6. General Comments. What do you think should be changed to improve future reports? (Indicate changes to organization, technical content, format, etc.) ________________________________

____

____

____

CURRENT ADDRESS

____
Organization

____
Name E-mail Name

____
Street or P.O. Box No.

____
City, State, Zip Code

7. If indicating a Change of Address or Address Correction, please provide the Current or Correct address above and the Old or Incorrect address below.

OLD ADDRESS

____
Organization

____
Name

____
Street or P.O. Box No.

____
City, State, Zip Code

(Remove this sheet, fold as indicated, tape closed, and mail.)

(DO NOT STAPLE)

DEPARTMENT OF THE ARMY

OFFICIAL BUSINESS

NO POSTAGE NECESSARY IF MAILED IN THE UNITED STATES

BUSINESS REPLY MAIL

FIRST CLASS PERMIT NO 0001,APG,MD

POSTAGE WILL BE PAID BY ADDRESSEE

DIRECTOR
US ARMY RESEARCH LABORATORY
ATTN AMSRL WM MB
ABERDEEN PROVING GROUND MD 21005-5069